General Disclaimer

One or more of the Following Statements may affect this Document

- This document has been reproduced from the best copy furnished by the organizational source. It is being released in the interest of making available as much information as possible.

- This document may contain data, which exceeds the sheet parameters. It was furnished in this condition by the organizational source and is the best copy available.

- This document may contain tone-on-tone or color graphs, charts and/or pictures, which have been reproduced in black and white.

- This document is paginated as submitted by the original source.

- Portions of this document are not fully legible due to the historical nature of some of the material. However, it is the best reproduction available from the original submission.

NAS 9-14808

ULTRASONIC CORONA SENSOR STUDY

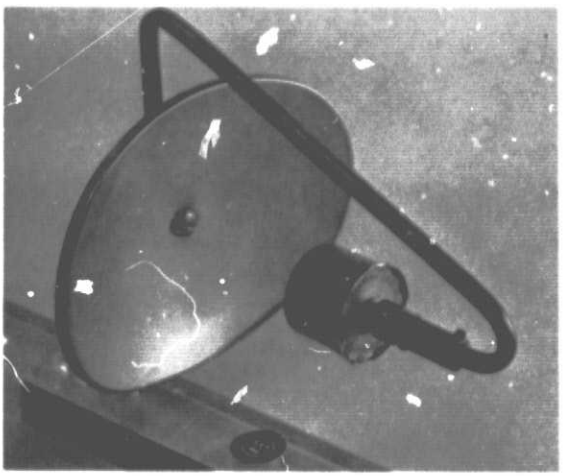

FINAL REPORT

HUD-10536-CE

Westinghouse Research Laboratories
Pittsburgh, Pennsylvania 15235

R. T. Harrold

April 28, 1976

Prepared for NASA Lyndon B. Johnson Space Center
Houston, Texas 77058

WESTINGHOUSE RESEARCH LABORATORIES
PITTSBURGH, PENNSYLVANIA 15235

CONTENTS

ULTRASONIC CORONA SENSOR STUDY

NAS 9-14808

FINAL REPORT -- APRIL 1976

R. T. Harrold

Westinghouse Research Laboratories
Pittsburgh, Pennsylvania 15235

1. OBJECTIVE

The overall objective of this program is to determine the feasibility of using ultrasonic (above 20 kHz) corona detection techniques to detect low order (non-arcing) coronas in varying degrees of vacuum within large high vacuum test chambers, and to design, fabricate, and deliver a prototype ultrasonic corona sensor.

2. SUMMARY

The feasibility of ultrasonically detecting low order (20 to 50 picocoulomb at atmospheric pressure) discharges in air has been demonstrated over a pressure range from atmospheric pressure down to about 5 Torr (the pressure nearly corresponding to 115,000 feet altitude). Detection is best achieved using a sensor frequency near 40 kHz, because the ultrasonic emissions (S) from typical discharges were found to be much lower at the higher frequencies ($S \propto f^{-4}$), and ambient noise is a problem at lower frequencies near 20 kHz, where the sensitivity is greater and detection below 0.1 Torr is possible.

In this study, a parabolic reflector was used to increase the detector sensitivity, but this was restricted to 10 centimeters in diameter

in the laboratory vacuum apparatus. It is anticipated that in large high vacuum test chambers a larger reflector would extend the useful operating range to a pressure of 1 Torr, or near an altitude of 150,000 feet.

There were no problems with the sensor materials outgassing and only a 40% reduction in sensitivity with high temperature operation to 66°C, but at -60°C the sensor response had fallen by 75% and at near -63°C it would not operate, presumably due to the inflexibility of the silicone rubber used to support the sensor crystal. However, the sensor was immersed several times in liquid nitrogen at -196°C and then returned to room temperature with no decline in performance. It is believed that the flexibility problem could be relieved to a certain extent by the use of polybutadiene crystal supports, as polybutadiene[1] has a glass transition temperature near -100°C, but the best approach would be to devise a crystal heating system. One possible way to heat the crystal may be to use artificial sunlight which would be focussed onto the crystal by the parabolic reflector.

Although in theory, the transmission of ultrasound in air is proportional to P (where P is pressure) in this study, at pressures below 100 Torr, the transmission at 41 kHz was found to be closely related to P^3. When this is considered together with the sonic emissions (S) from typical discharges falling with increasing frequency (f), $S \propto f^{-4}$, ultrasonic detection much below about 1 Torr pressure appears unlikely for routine discharge detection, even if techniques to extract the sonic signal from noise were used.

However, the useful pressure range of the 41 kHz parabolic microphone does include the critical region of large glow coronas, from about 200 Torr to 5 Torr, where there is a large increase and then decrease in discharge magnitude. It is likely that ultraviolet corona sensors can also be used in this pressure range and below, but the parabolic microphone is highly directional, which is helpful for pinpointing a corona discharge, and from the experimental data it is estimated that discharges external to the apparatus under test, and having a magnitude

in the 20 to 50 picocoulomb range at atmospheric pressure, can be ultrasonically detected at a distance of one meter over the range of lower pressures to about 5 Torr.

It is recommended that any further work on this project should be directed toward the development of simple radar-type of display devices that would give a map of the discharge sites on the test object; and also the apparent absence of attenuation of 20 kHz ultrasound at low pressure should be investigated.

3. INTRODUCTION

Although large order (10,000 picocoulomb) corona discharges in air can be heard by ear and observed by eye in the dark, the detection and location of low order (20 to 50 picocoulomb) discharges associated with high voltage electrical apparatus in air can present some very formidable problems. The masking of corona signals by interference, attenuation of signals between the discharge site and detector location, unwanted discharge signals from the high voltage test apparatus, and multiple corona sources, can make corona detection and location difficult. Numerous different types of corona sensors are available, ranging from electromagnetic and ultrasonic, to ultraviolet, all of which are helpful, but often considerable experience is needed to correctly interpret the data measured.

Electrical discharges at low pressure and vacuum are unique, in that the electrical pulse from a small discharge at a point in air at atmospheric pressure may enlarge ten to one hundred times in the glow region when the pressure is reduced to approximately 50 Torr, and then fall to near its original size at lower pressures in the 1 Torr range. In the glow region, the point discharge has the appearance of slightly wandering multiple ribbons of blue light extending to grounded regions, and the tendency is for the discharges to spread over a large volume of the vacuum

chamber, provided the power supply can furnish the necessary current. Obviously, ultraviolet sensors could be used for detecting these types of coronas, but with the spreading discharge it may be difficult to pinpoint the discharge location. It is not so obvious that ultrasonic sensors could be applied to the detection of these low pressure discharges, and the main objective of this present study is to determine the feasibility of this approach.

The scope of the work reported here covers the relationship between the electrical pulse charge and ultrasonic emissions from different discharges in varying degrees of vacuum. Also, the ultrasonic spectrum signatures of these discharges; attenuation/distance/pressure relationships, and the design and performance of a parabolic microphone for use in large high vacuum test chambers. The characteristics and useful practical operating range of this sensor are outlined and recommendations made for further work.

4. LITERATURE SURVEY

It is believed that this present study is the first concerned with the ultrasonic emissions from electrical discharges at low pressure, and a recent literature search has reinforced this belief.

The survey was carried out using a teletype terminal linked to the National Technical Information Service, and a rapid search was made of Government reports since 1964, as well as Physics Abstracts, Engineering Index and Electrical and Electronic Engineering Abstracts dating from 1958. A few useful papers were located and these are listed in Appendix I. The most pertinent and useful reference is the following:

> "Sound Propagation in Rarefied Gases," by Bolt Beranek and Newman, Inc., Cambridge, Mass., Report No. bbn-1169 for U.S.G.R.D.R., November 1964.

5. THEORETICAL CONSIDERATIONS

Prior to this study, from theoretical considerations, because sound velocity is pressure independent[2], ultrasound transmission at low pressures was anticipated, although it was realized that the effect of reduced pressure to attenuate gas transmitted ultrasound could be a serious problem, as transmission is directly proportional[2] to gas density. Also, it was known that attenuation of soundwaves in air increased very much with increasing frequency, and the ultrasonic emissions from some discharge sources reduced considerably at higher frequencies, and for these reasons it was thought that the best choice for the sensor frequency was probably in the 30 to 40 kHz range. During this study, these beliefs were generally confirmed, and it was also realized that sound transmission in a gas is linked to the mean free path between molecular collisions, and consequently, soundwave transmission was probably not possible below certain pressures.

These theoretical considerations are briefly outlined below:

5.1 Transmission of Ultrasound in Air

The velocity of sound in a gas, such as air, is proportional[2] to $\sqrt{\frac{\gamma P}{\rho}}$, where γ is the ratio of principal specific heats, P the pressure, and ρ the density. As $\rho = m/v$, where m is mass and v is volume, and $Pv = mRT$, where R is a gas constant, it follows that velocity is proportional to $\sqrt{T}$, where T is the absolute temperature. Therefore, the velocity of sound in air is independent of pressure, which infers there is sound transmission at low pressure.

5.2 Attenuation of Ultrasound in Air

Generally, if a site of ultrasonic emissions is a point source, then, the sound pressure level[2] at a detector located at distance d is proportional to d^{-1}. Apart from attenuation with distance, soundwaves experience considerable attenuation with increasing frequency, f, and attenuation[2] in air, in decibels per foot, is approximately proportional

to f^2. For these reasons, ultrasonic measurements in air can be more readily made at frequencies below ~40 kHz rather than higher frequencies. The effect of reduced pressure on the transmission of ultrasound in a gas can be a serious problem as the transmission is proportional[2] to gas density.

5.3 Ultrasonic Frequency Spectra of Air Discharges

It is believed that the ultrasonic emissions from many types of corona discharges in air fall in magnitude with increasing frequency, which is the reason why sonic sensors for localizing troublesome discharge sources associated with high voltage power lines operate in the 20 to 40 kHz range, but there is little published information regarding the frequency spectra. Data taken by Allan and Kashani[3] demonstrates that the ultrasonic spectra of discharges from an electrically stressed bare conductor falls considerably between 10 and 50 kHz. Also, a study by Heroux and Trinh[4] indicates that the spectrum of discharges from a positive cone falls with increasing frequency.

5.4 Low Pressure Limit of Ultrasound Wave Transmission

As ultrasound wave transmission in air depends on molecules striking molecules, it follows that, as the pressure is reduced, wave transmission is not possible when the mean-free-path between molecular collisions is greater than the ultrasound wavelength. For the sensor frequencies used in this study, 21 kHz, 41 kHz and 77 kHz, the respective limiting pressures are estimated to be approximately 3×10^{-3} Torr, 5.5×10^{-3} Torr and 1.2×10^{-2} Torr. Obviously, at lower pressures, lower ultrasound frequencies are required for wave transmission.

At pressures where wave transmission is not possible, sound transmission is in the geometrical relaxation regime[5] where molecules travel from the sound transmitter to receiver with few collisions.

6. EXPERIMENTAL APPARATUS AND INSTRUMENTATION

A schematic of the apparatus and instrumentation for monitoring the acoustic emissions from electrical discharges at low pressure and vacuum is given in Fig. 1. Basically, the apparatus consists of a Plexiglas cylinder of approximately 13 cm inside diameter and 61 cm in length, sealed at the ends by either brass or Plexiglas plates and o-rings. At one end of the cylinder, different electrical discharge sources may be placed and energized, while at the opposite end, different frequency sonic sensors can be located up to a maximum distance of 0.5 meters from the discharge site. Connections through the end plates allow the application of high voltage, the evacuation of the cylinder, and the transmission of the electrical and acoustical signals from inside the cylinder to the external instrumentation. Several vacuum gauges were used to measure air pressure, and these included two Wallace and Tierman, pennwalt model, absolute pressure gauges, Oto 800 Torr and 0 to 50 Torr, a thermocouple gauge and a Phillips gauge, type PHG-09.

The electrical pulses from the discharges are measured in picocoulombs and viewed oscillographically so that their phase relationship with the 60 Hz applied voltage may be observed. In addition, the discharge site is viewed in the dark through a telescope to allow light emissions to be observed.

Acoustic emissions in microvolts quasipeak (μVQP) are detected via resonant transducers of approximately 20 kHz, 40 kHz and 70 kHz frequency, an impedance matching (10 MΩ to 50 Ω) amplifier and a narrow band tunable amplifier with an indicating meter (Singer-Stoddart NM 12T radio noise meter). The sonic sensors are shielded from electrical induced noise, and the amplifiers battery operated and isolated from ground. To help in identification, the delayed sonic signals can be oscillographically displayed together with the electrical pulses from a discharge. In order to verify that the sonic emissions detected were valid and not influenced by electrical induced noise, each test would be repeated with the sonic sensor acoustically shielded.

Many experimental parameters were also evaluated using a pulsed ultrasound source instead of a discharge source.

6.1 Calibration of Microphones

The sensitivities of the 21, 41 and 77 kHz microphones used in this study were measured in the Acoustic Laboratory in atmospheric air with the following results:

21 kHz . . . . . 250 μV/μbar.
41 kHz . . . . . 1000 μV/μbar.
77 kHz . . . . . 850 μV/μbar.

In this report, the data used in the graphical comparison of the 21 kHz, 41 kHz and 77 kHz ultrasonic emissions have been normalized to the sensitivity of the 41 kHz sensor.

7. GENERAL EXPERIMENTAL PROCEDURE

7.1 Electrical Discharges

With a sonic sensor located approximately 40 cms from a particular discharge source, energized at a particular voltage, measurements would be made of the range of electrical pulse charge, the sonic signal, the pressure, and the discharge (60 Hz) voltage and current, as the pressure was reduced from atmospheric to that at which sonic emissions could not be detected. Measurements were made at approximate two minute intervals to ensure that the pressure in the cylinder equalled that read by the pressure gauge, which was located away from the cylinder. This experimental procedure was repeated with different frequency sensors located at various distances from the discharge source, and also with acoustic shielding of the sensor in order to ensure the measurement validity.

It was necessary to isolate the sonic sensor from ground to prevent electrical induced noise problems, but unfortunately, in the 0.2 Torr pressure range, due to the spreading of the glow discharge, the sonic sensor system would charge to high voltage and give ambiguous readings. Consequently, to

obtain better data regarding the ultrasound characteristics at these pressures, it was necessary to use a pulsed ultrasonic microphone as a transmitter to check the operating characteristics of the system.

7.2 Pulsed Ultrasound

The microphones were used as sources of pulsed ultrasound by incorporating them into relaxation oscillator circuits, and in this way, unlike the ultrasonic emissions from corona discharges which change considerably with pressure, the constant amplitude pulses from the microphones were ideal for examining the characteristics of sound transmission in low pressure air. As the microphones represented capacitances in the 600-1200 pF range, by charging through a 10 megohm resistor to an appropriate voltage and discharging through a parallel connected Siemens gas gap, relaxation oscillators were formed which emitted ultrasonic pulses at a rate near 100 per second. Several different voltages were used at the different sonic frequencies as follows in Table I:

TABLE I

ULTRASONIC PULSE SYSTEMS

		Pulses Per Second at Different Gap Voltages		
Sensor	Capacitance	90 V	230 V	800 V
21 kHz	∿1200 pF	∿125 pps	∿75 pps	∿17 pps
41 kHz	∿1500 pF	∿75	∿40	∿10
77 kHz	∿ 600 pF	∿220	∿140	∿30

Using a pulsed ultrasound system it was especially necessary to wait two minutes between measurements, since at the lower pressures the ultrasonic crystal could easily overheat. Although the 800 volt system gave the largest ultrasonic pulse and allowed measurements to be made over a wide pressure range, it was necessary to check the trend of these measurements with the lower pulse voltages, because 800 volts is above the Paschen minimum (250 V) for air.

Other experimental procedures, such as those used at low temperature and in the anechoic chamber will be described later.

8. EXPERIMENTAL RESULTS

8.1 Ultrasound/Electrical Pulse Charge/Pressure

8.1.1 Discharges from a Point Stressed at 2.8 kV_{rms} and Spaced 1 mm Above an Insulated Plane

The changes in electrical pulse amplitude and quantity as the pressure is reduced are shown in Fig. 2, while the variations of ultrasonic emissions at 21 kHz, 41 kHz and 73.5 kHz from a point discharge in varying degrees of vacuum are illustrated in Figs. 3, 4 and 5. Similar patterns are observed at each frequency with peak acoustic emissions occurring in the glow region near 20 Torr. In Fig. 6, a plot of sonic emissions versus pressure reveals, for the detection system used, that acoustic signals were not detected at pressures below 5 Torr pressure at 73.5 kHz, 1 Torr at 41 kHz, and 0.2 Torr at 21 kHz (the spreading discharge prevented accurate readings at lower pressures).

8.1.2 Discharges from a 2.5 cm Diameter Sphere Stressed at 4.2 kV_{rms} and Spaced 0.1 mm above an Insulated Plane

The changes in electrical pulse amplitude and quantity as the pressure is reduced are shown in Fig. 2, while the variations of ultrasonic emissions at 21 kHz, 41 kHz and 73.5 kHz for discharges from a sphere in varying degrees of vacuum are illustrated in Figs. 7, 8 and 9. Similar patterns are observed at each frequency with peak acoustic emissions occurring near 50 Torr in the glow region. In Fig. 10, a plot of sonic emissions versus pressure reveals, for the detection system used, that acoustic signals were detected at pressures of 10 Torr for 73.5 kHz, 5 Torr for 41 kHz, and 0.2 Torr for 21 kHz. From the 21 kHz data, it is estimated that sonic emissions would still be monitored at 0.01 Torr.

8.2 Ultrasonic Frequency Spectra/Pressure

The frequency (f) spectrum from 20 to ~80 kHz of the ultrasonic emissions from an electrically stressed point above an insulated plane, Fig. 11, is roughly related to f^{-2} near atmospheric pressure, but this gradually changes to an f^{-4} relationship as the pressure is reduced to near one Torr. Where discharges are associated with a sphere above an insulated plane, Fig. 12, the f^{-4} relationship generally holds for the ultrasonic emissions over a pressure range from atmospheric to 5 Torr.

8.3 Attenuation/Distance/Pressure

It was inaccurate to measure the attenuation with distance of ultrasound in the vacuum cylinder, due to the difficulty of aligning the relatively narrow beam sensors with the sonic emissions from the electrical discharge. For this reason, attenuation was measured using the microphones as pulsed sources of ultrasound, Table II.

TABLE II
ATTENUATION OF PULSED ULTRASOUND IN VARYING DEGREES OF VACUUM

	Attenuation in Decibels				
Pressure Torr	41 kHz 230 Volt Pulse 5 to 25 cm	41 kHz 800 Volt Pulse 5 to 25 cm	41 kHz with Reflector 90 Volt Pulse 25 to 50 cm	77.7 kHz 90 Volt Pulse 10 to 40 cm	77.7 kHz 800 Volt Pulse 10 to 40 cm
730	16.0 dB	13.4 dB	3.7 dB	5.2 dB	5.2 dB
500	17.0	13.0	3.4	5.9	6.7
300	17.7	12.0	5.0	6.7	7.6
100	19.5	12.0	4.5	8.3	9.3
50	19.0	15.5	2.6	7.1	12.0
20	18.2	14.0	7.3	---	16.8
10	19.2	12.0	---	---	16.0
5	---	15.0	---	---	---
1	---	---	---	---	---

Some of these results indicate a reasonable agreement with theory, e.g., at 41 kHz over a distance change of five times, a 14 dB attenuation would be expected. From Table II, the attenuation at 730 Torr is 16 dB, with an increase to 19.2 dB at 10 Torr. Generally, a slight increase in attenuation was noted as the pressure was reduced.

Attenuation measurements were not accurate at 21 kHz due to reflections of sonic waves from the cylinder walls and this problem was also apparent at the other frequencies, see Fig. 13, which illustrates both the attenuation of 41 kHz waves within a cylinder and without an enclosure. This means the attenuation values in Table II can only be considered approximate.

As the pressure was reduced, the transmission of ultrasound at a frequency of 41 kHz reduced considerably more than anticipated, see Fig. 14. In theory, the transmission should reduce directly in proportion to pressure,[2] but in Fig. 14, it can be seen that at 41 kHz the transmission is related to P^1 to P^2 in the 760 to 100 Torr range, and P^2 to P^3 in the region below 100 Torr. At 21 kHz there appears to be little reduction in transmission at pressures from about 20 Torr to 0.003 Torr.

9. PRELIMINARY DISCUSSION

The results presented so far indicate a certain agreement with theory and exhibit trends similar to those anticipated. However, the amplitude of the ultrasonic emissions from the typical discharges fell with increasing frequency by a factor proportional to f^{-4}, and the magnitude of the 41 kHz ultrasonic signals decreased at the lower (<100 Torr) pressures (P) by a factor approximately proportional to between P^2 and P^4, rather than P^1. These relationships suggest the routine use of ultrasonic corona sensors below 10 Torr pressure will be difficult, but with a parabolic reflector to increase the detector sensitivity, a practical system

is envisaged. Surprisingly, it appears that sonic emissions at 21 kHz do not attenuate much below 20 Torr pressure as similar readings were also recorded at 0.003 Torr, but this needs further investigation and confirmation.

It is believed that a sensor frequency near 40 kHz is optimum, as frequencies near 20 kHz are subject to ambient noise interference, and at higher frequencies the sonic emissions from typical discharges fall considerably. With 40 kHz selected for the sensor frequency, the next phase of this study involved the design of a parabolic microphone.

10. DESIGN AND CONSTRUCTION OF PARABOLIC MICROPHONE

The principle of these microphones is that soundwaves striking the parabolic surface will be reflected to converge on the microphone crystal which is located at the parabola focus. An increased gain proportional to the ratio of parabola and crystal surface areas should result. With the laboratory vacuum system used in this study, it was necessary to limit the parabola diameter to approximately 10 cm, and for convenience, a 10 cm diameter nickel plated steel reflector from a solar cigarette lighter was combined with a 40 kHz microphone to yield an effective higher gain sensor. The sensor design is illustrated in Fig. 15 and a picture of the device is shown in Fig. 16.

10.1 Sensor Materials Exposed to Vacuum Environment

The approximate weights of the sensor materials are listed in Table III.

10.2 Outgassing Characteristics

The majority of the sensor materials, Table III, fall in the category recommended[6] for vacuum use, and with the 41 kHz parabolic microphone stored in a 0.001 Torr atmosphere for several hours, no pressure changes were observed.

TABLE III

SENSOR MATERIALS AND WEIGHTS

Part No.		
[1]	Parabolic reflector -- steel, with nickel/chrome plate. .	25.52 grammes
[2]	Aluminum tubing, 4.8 mm diameter.	7.00
[3]	Aluminum support block, 2.5 x 2.5 x 1.25 cm	17.63
[4]	Tin plated brass spacer, 12.7 mm diameter	1.60
[5]	Stranded copper wire, plastic coated (PVC).	1.06
[6]	Stainless steel nut, 6-32	0.82
[7]	Two nickel plated brass angle brackets.	1.54
[8]	Three stainless steel screws, 6-32 by 6.35 mm	2.18
[9]	One stainless steel set screw, 4-40 by 3.2 mm	0.09
[10]	Two stainless steel set screws, 6-32 by 3.2 mm.	0.23
[11]	BNC connector (Teflon, plated brass, silver plated pin, nickel plated case)	5.57
[12]	Nickel plated brass shaft adaptor, 6.35 mm diameter . . .	6.64
[13]	Phono plug of tin plated brass and micarta.	1.40
[14]	Brass tubing, 8 mm O.D. x 5 mm I.D. x 15 mm	3.14
[15]	Four stainless steel lock washers, number 6	0.50
[16]	Microphone, 41 kHz.	7.12
[17]	Brass lock washer, 6-32	0.12
[18]	Solder, 60/40, tin/lead	0.20
	TOTAL	82.46 grammes

Microphone		
	Aluminum case	2.10 grammes
	Aluminum screen	0.20
	Crystal, lead titanate/lead zirconate	0.30
	Copper wire	0.01
	Brass	0.10
	Micarta mount	0.40
	Steel phono plug and tin plated mounting bracket.	4.00
	Silicone rubber beads supporting crystal.	0.01
	TOTAL	7.12 grammes

11. PERFORMANCE OF PARABOLIC MICROPHONE

The characteristics of the parabolic microphone are outlined below:

11.1 Sensitivity Versus Pressure

In Fig. 17, the variation of the 41 kHz sonic signal received at 25 cm from a 41 kHz microphone pulsed at 800 volts is indicated over a pressure range from atmospheric to 5 Torr. Two curves are displayed, one for a 41 kHz microphone alone, and one for the same microphone with the addition of the parabolic reflector. The gain using the reflector is about 2.5, and this can be interpreted in terms of reflectivity relative to that at atmospheric pressure, as indicated. It is apparent that the reflection factor is substantially constant over a pressure range from atmospheric to 10 Torr, and although less reflectivity is indicated at 5 Torr, this is probably an inaccurate reading as it was taken at signal levels near the receiver noise level. Apart from the reflectivity readings, the most important aspect of these curves is the rapid reduction in the received signal level (proportional to P^3) over the 100 to 5 Torr pressure region.

11.2 Sensitivity to Pulsed Ultrasonic Beam

The gain of the parabolic microphone was checked in air at one atmosphere, using a 41 kHz microphone pulsed with 90 volt pulses as a sound source, at a distance of 44 cm. With the spacing of 44 cm between the transmitting crystal (0.5 cm from microphone mesh screen) and receiving crystal, the two microphones would be orientated for maximum receiver response as recorded via a Tektronix 1A7A amplifier and 556 oscilloscope. The receiving microphone would then be placed at the focal point of the 10 cm parabolic reflector and adjusted for maximum response with the total soundwave travel path from transmitter to the reflector and back to the receiving crystal still 44 cm. Values of gain near 2.5 (8 dB) were found as outlined in Table IV, where the results using several identical 41 kHz microphones are listed.

TABLE IV

MEASUREMENTS OF PARABOLIC MICROPHONE GAIN USING PULSED ULTRASONIC BEAM

Transmitting Microphone No. 4 -- 41 kHz
Pulsed at 100 pps 90 Volts - Distance transmitter to receiver 44 cm.

Receiving Microphone No.	Peak Signal Received Without Reflector mV	Peak Signal Received with Parabolic Rellector mV	Gain
1	7.0	16.0	(7.2 dB) 2.30
8	8.0	20.0	(8.0 dB) 2.50
9	9.0	22.0	(7.8 dB) 2.45
10	8.0	18.0	(7.0 dB) 2.25
11	8.0	20.0	(8.0 dB) 2.50
12	8.0	17.0	(6.6 dB) 2.13

Theoretically, on an area basis, approximately 50 cm^2 for the reflector surface and near 1 cm^2 for the crystal, a gain near 50 (instead of 2.5) would be expected, but it is believed that the large microphone size relative to the reflector diameter shields a considerable portion of any incoming soundwaves, especially with the narrow beam used. It was reasoned that a larger gain should result using a spark source, and this was tried next.

11.3 Sensitivity to a Spark Source

A similar procedure to that used with the pulse source was followed using the spark, except the distance between the spark and receiving microphone was 1 meter. The following data were obtained regarding the gain of the parabolic microphone:

TABLE V

MEASUREMENTS OF PARABOLIC MICROPHONE GAIN USING SPARK SOURCE

Spark Source -- Approximate 2 mil gap between 1 cm diameter brass spheres, 50 pF parallel capacitor charged through 10 MΩ resistor and discharged through the gap and 10 Ω resistor. Approx. 125 pps, 1000 V applied. Distance spark gap to microphone, 1 meter.

Receiving Microphone No.	Peak Signal Received Without Reflector mV	Peak Signal Received With Parabolic Reflector mV	Gain
10	3.70	15.50	4.18 [12.4 dB]
11	4.25	17.00	4.00 [12.00 dB]
12	3.70	16.50	4.46 [13.0 dB]

As expected, the parabolic microphone exhibits higher gain when receiving ultrasonic emissions from a spark source, compared with the gain when a narrow pulsed sonic beam is used.

11.4 Operation Over Temperature Range -184°C (-300°F) to +60°C (+150°F)

Experiments over a wide temperature range were carried out with a 41 kHz receiving microphone located within a small metal box with a thermometer to record air temperature and a one inch aperture in the wall, so that sound transmitted from an externally located pulsed microphone would reach the internal microphone. The crystals of the two microphones were 12.5 cm apart and the external 41 kHz microphone was pulsed at 90 volts and 75 pps. Calcium sulfate crystals were placed within the box to help keep the air dry during the experiments.

The signal received by the microphone, as measured by the radio noise meter and the oscilloscope, was noted at room temperature and the changes in signal level recorded as the microphone was heated to 70°C using

a hot air blower. Low temperature readings were made to -63°C using solid carbon dioxide applied to the metal box.

At +70°C the receiver sensitivity had fallen by about 40%, while at -60°C it had reduced by 75%, and almost ceased functioning at -63°C. It is believed that this is due to the silicone rubber supports of the microphone crystal becoming inflexible at -63°C and the use of polybutadiene,[1] which has a glass transition temperature of -102°C, would help alleviate this problem. However, the microphone suffered no damage over this temperature range and also performed satisfactorily at room temperature after repeated immersion for five minutes at a time in liquid nitrogen at -196°C. Also, it is likely that some of the soundwaves were deflected away from the microphone at the interface of the warm and cold air (the transmitting microphone was in room temperature air), giving a poorer impression of the receiving microphone performance.

11.5 Directivity

The directivity of the parabolic microphone was obtained in an anechoic chamber where the microphone could be rotated and a graphical record of its output made using the radio noise meter as a receiver. With the microphone 2.25 meters from a Brüel and Kjaev condenser microphone type 4145 which was used as a transmitter, the directivity pattern of Fig. 18 was obtained. It will be observed that the device is highly directive with a beam angle of about 25°.

11.6 Frequency Response

The frequency response was also measured in the anechoic chamber, simply by tuning the narrowband noise meter used as a receiver and recording the result as in Fig. 19. It will be noted that the parabolic microphone response peaks at 41.5 kHz and the 6 dB bandwidth is approximately 2.7 kHz.

11.7 Sensitivity

Using a Brüel and Kjaev type 4136 condenser microphone as a calibrated probe, by substitution in the sound field of the Brüel and Kjaev type 4145 microphone used as a transmitter, the sensitivity of the parabolic microphone was determined to be close to 2000 μV/μbar.

11.8 Attenuation

In the anechoic chamber, there was sufficient space to move the parabolic microphone to a distance of 3 meters from the transmitting microphone, which was assumed to be a spherical sound source. Attenuation measurements over a distance range from 30 cm to 3 meters, Fig. 20, reveals a change with distance (d) closely related to d^{-1}.

11.9 Selectivity

The 40 kHz operating frequency chosen for the ultrasonic sensor is a compromise, because although greater sensitivity to electrical discharges is possible at 20 kHz, ambient noise at the lower frequency would be a big problem. On the other hand, ambient noise would be very little at frequencies near 70 kHz, but the sensitivity to ultrasonic emissions from discharges would be less.

As a selectivity test, a quarter (25¢) was dropped onto a solid surface from a height of 10 cm with the 40 kHz parabolic microphone 1 meter distance and a transient reading of 40 to 100 μV was recorded. A 2 watt, 6 inch diameter refrigerator fan operating 1 meter from the microphone indicated no meter reading above ambient (0.4 μV), while a 5 ampere toggle switch operated at 1 meter distance gave 20 to 50 μV. These readings should be compared with measurements of 1 to 150 μV, obtained from discharges in the atmospheric pressure to 20 Torr range. Transient noises are not expected to be troublesome as they should be distinguishable from the regularly repeated ultrasonic emissions from electrical discharges.

12. OVERALL DISCUSSION

This study has demonstrated that the 41 kHz parabolic microphone is highly directional and sensitive enough to detect the ultrasonic emissions from low order (20-50 pC at atmospheric pressure) electrical discharges in the pressure range from atmospheric to about 5 Torr, at a distance of ~0.5 meters. In large high vacuum test chambers, a much larger diameter parabolic reflector could be used which would have higher gain, and it is estimated that if a larger diameter parabolic reflector increased the microphone gain by a factor of 20, then, low order discharges would be detectable at a distance of 10 meters and over a pressure range from atmospheric to 5 Torr. However, because of the rapid decrease in the level of the 41 kHz acoustic emissions from discharges as the pressure is lowered (proportional to P^2 to P^4), it is doubtful whether the useful operating range of the sensor would be extended much below 1 Torr. It was found that a sensor frequency near 40 kHz is best because the ultrasonic emissions (S) from typical discharges were found to be much lower at higher frequencies ($S \propto f^{-4}$), and ambient noise is a problem at lower frequencies near 20 kHz. With the high directivity of the sensor, if it were mounted in the fashion of a radar antenna, it should be possible to pinpoint a site of ultrasonic emissions.

With the present sensor design, useful operation is possible over a temperature range from approximately +70°C to -40°C, and the device withstood -196°C without damage. It is believed that the sensor may be modified for lower temperature operation by replacement of the silicone rubber crystal supports which become inflexible at -63°C. The sensor is constructed of materials compatible with a vacuum environment and no outgassing problems were found.

The use of simulated sunlight near the sensor reflector could cause the crystal to overheat, and if necessary, the shiny reflector could be blackened as it would still reflect soundwaves. With the present design of parabolic microphone, it is a simple matter to change the

operating frequency, because the microphone can be easily removed and one of a different frequency plugged-in.

13. RECOMMENDATIONS FOR FURTHER STUDY

Although the 41 kHz parabolic microphone appears adequate for sensing discharges within large vacuum test chambers, as with all corona detection devices, the interpretation of the measurements is extremely important. For this reason, the most important part of future work would be the development of simple display devices, operable by semi-skilled personnel, to show a map of the discharge regions of the test object. This could take the form of a radar-type of display with the sensor mounted for remote scanning. The addition of a closed circuit television display and a beam of light from the sensor position and paralleling the received sonic beam, would help in identifying and locating the electrical discharge sites on the test object.

Another approach for the ultrasonic detection and location of low value discharges at low pressure would be to use small diameter tubes to guide the sonic waves to the sensor. It is likely that with the use of sonic waveguides, a very sensitive system would result, as we have found during laboratory experiments using a spark in air and a one inch diameter pipe, a 10 times increase in received signal at a distance of 2 meters. Although a system of this nature seems unwieldy, it is believed that a simple practical detector could be developed using lightweight telescoping insulating tubes mounted on a scanning fixture, and operated remotely so as to extend and retract in a similar manner to an automobile antenna, in order to zero in on the ultrasonic emissions from a discharge site.

Ultimately, it is believed that by combining the sonic sensor with an ultraviolet sensor, together with a closed circuit television system, a very versatile and easy to use discharge detection and location system could be devised. One way to achieve this would be to mount

adjacent to each other, on a remotely controlled scanning platform within a vacuum test chamber, three sensors. One would be a parabolic microphone (as developed in this present study), one a small ultraviolet sensor which operates in the solar blind region, and one a vidicon T.V. camera tube with maximum response to green light. With the inside of the chamber light illuminated and the test object within energized at high voltage, the signals from each sensor would be transmitted to an externally located color television receiver. The signal from the T.V. camera would be applied to the green gun only, so that a green picture of the test object within the chamber would be seen, while the signal from the sonic sensor would be applied to the grid of the red gun, so that red regions on the T.V. picture would indicate sites of ultrasonic emissions from the test object. The signals from the ultraviolet sensor would be applied to the blue gun only, and consequently, ultraviolet emissions or the location of wandering streamer type of discharges associated with the test object, would be observed in blue on the T.V. picture.

This technique has the advantages of dual discharge detection, together with a coarse (ultraviolet from wandering streamers), and fine (highly directional sonic sensor), discharge location capability, and in one picture the test object can be seen and discharge sites observed, as the pressure within the chamber is varied. In addition, video tape recording could be used to reduce the test time involved when a discharge is being located.

Also, the apparent zero attenuation of 20 kHz signals in the 10 Torr to 0.003 Torr region should be investigated, because, if understood, the development of more sensitive ultrasonic corona sensors may be possible.

14. REFERENCES

1. Polymer Handbook, J. Brandrup and E. H. Immergut, published by John Wiley and Sons, New York, 1966.

2. American Institute of Physics Handbook, Dwight E. Gray, Editor, McGraw Hill Book Co., New York, 1957.

3. Allan and Kashani, "Location and Measurement of Radio Noise Using an Ultrasonic Detector," IEE Conf. on Diagnostic Testing of High Voltage Power Apparatus in Service, London, March 1973.

4. Heroux and Trinh, "A Statistical Study of Electrical and Acoustical Characteristics of Pulsative Corona," IEEE Conf. Paper A76 122-2, at 1976 Winter Power Meeting.

5. "Sound Propagation in Rarefied Gases," by Bolt Beranek and Newman, Inc., Cambridge, Mass., Report No. bbn-1169 for U.S.G.R.D.R., November 1964.

6. C. E. Jahnke, "Materials for the Space Vacuum," Space Aeronautics, 1964, pp. 89-91.

15. APPENDIX I -- LITERATURE SURVEY

The literature survey yielded the following pertinent papers:

[i] "Sound Propagation in Rarefied Gases," by Bolt Beranek and Newman, Inc., Cambridge, Mass., Report No. bbn-1169 for U.S.G.R.D.R., November 1964.

[ii] "Sonic Boom Propagation in Stratified Atmosphere with Computer Program," by W. D. Hayes, et al., NASA Report No. NASA-CR-1299, April 1969.

[iii] "Method of Monitoring the Physiochemical Parameters of Media," by N. I. Mozhenin, et al., IZMER TEKH (USSR), Vol. 16, No. 5, 76-7, May 1973.

[iv] "Generation and Detection of Acoustic Waves in Pulsed Electrical Discharges," K. J. Nygaard and G. Meltz, Journal of the Acoustic Society of America, Vol. 44, No. 6, pp. 1566-1569, 1968.

16. ACKNOWLEDGMENT

The author would like to acknowledge the help of Dr. A. E. Hribar and R. A. Warren of the Acoustics Laboratory where the characteristics of the parabolic microphone were measured.

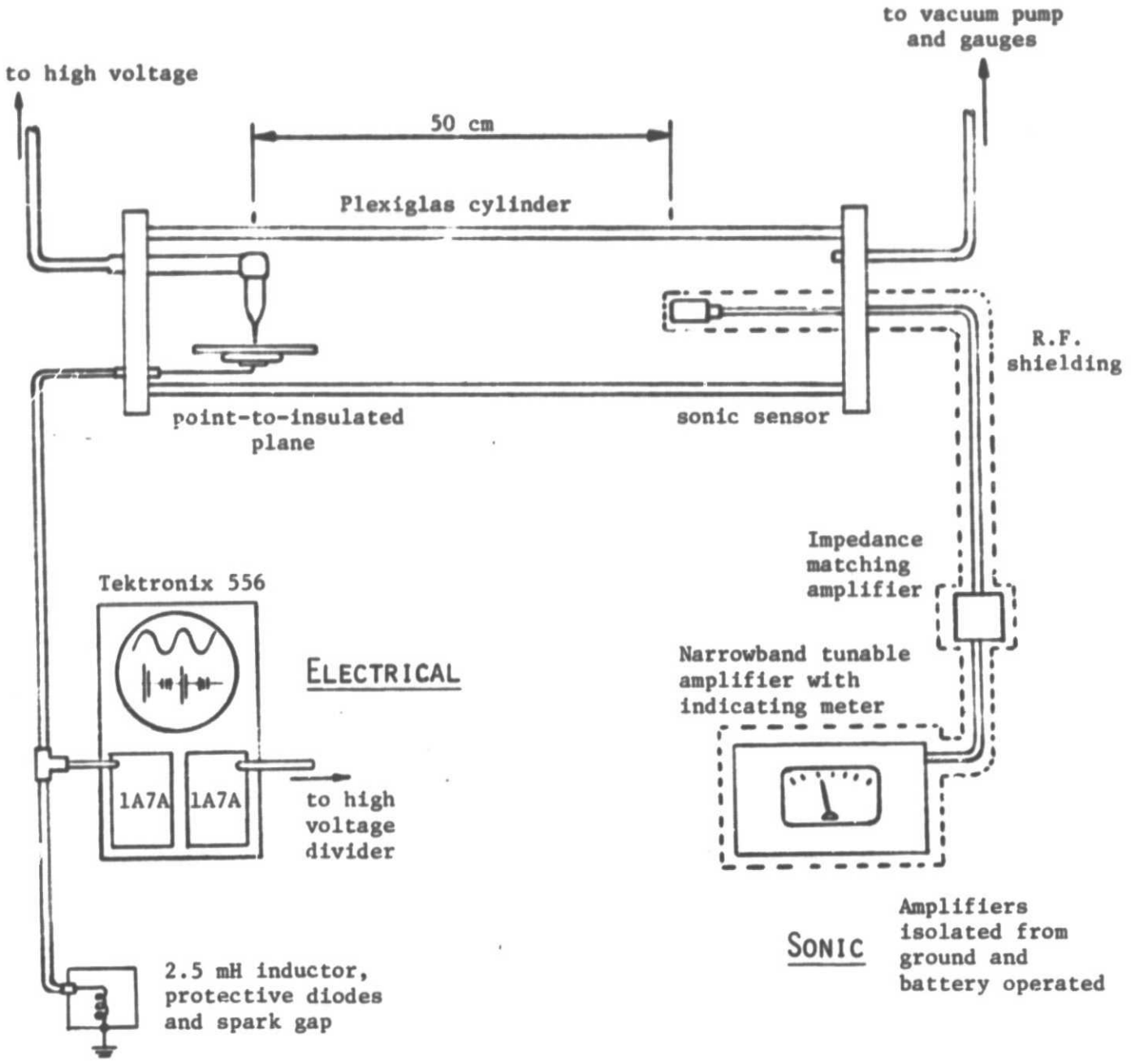

FIG. 1 - SCHEMATIC OF APPARATUS AND INSTRUMENTATION FOR MONITORING THE ACOUSTIC EMISSIONS FROM ELECTRICAL DISCHARGES AT LOW PRESSURE AND VACUUM

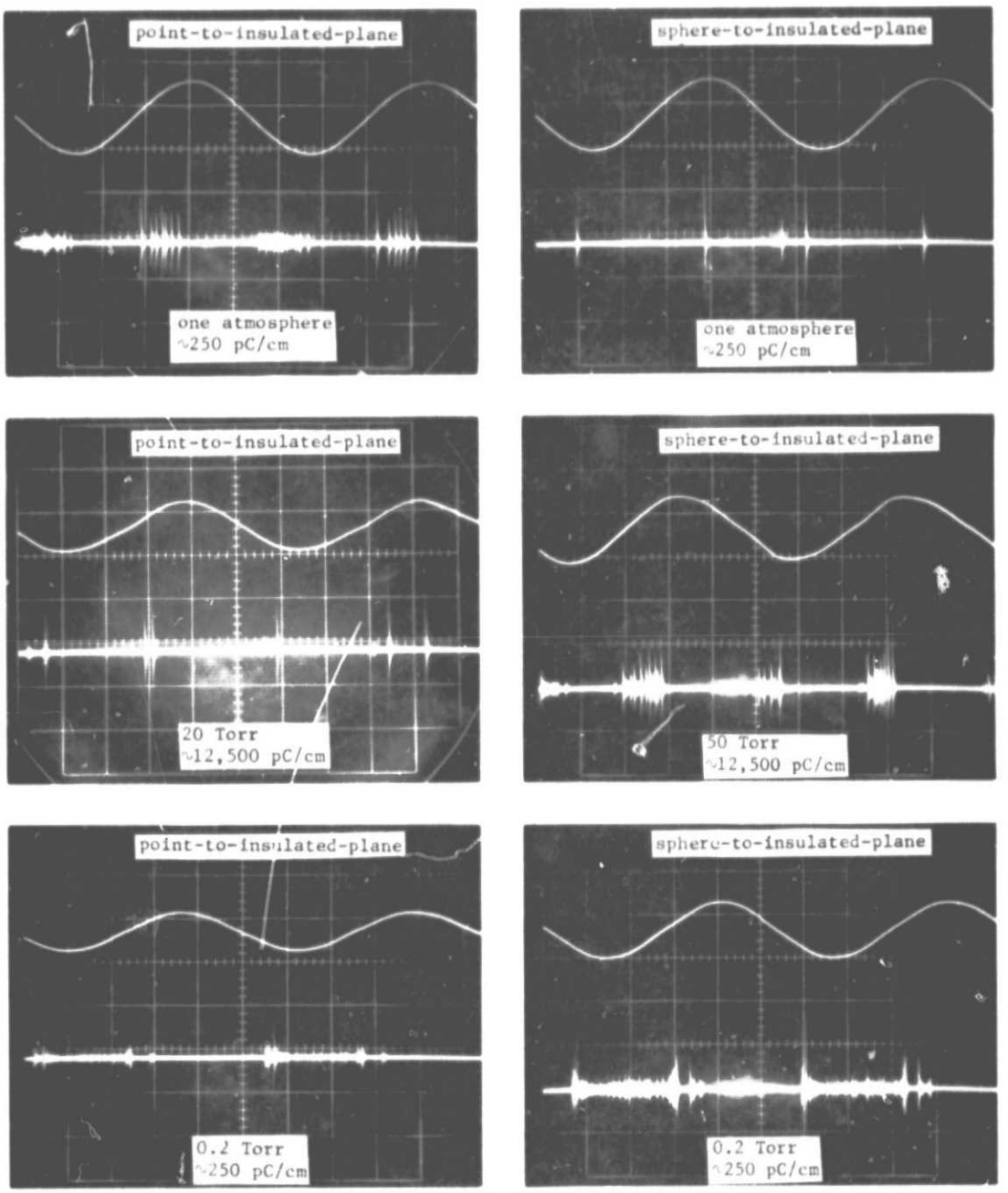

point 1 mm above an insulated plane and stressed at 2.8 kV when at 1 atmosphere

2.5 cm dia sphere spaced 0.1 mm from an insulated plane and stressed at 4.2 kV when at 1 atmos.

Fig. 2 -- Phase relationships between the electrical discharge pulses and applied 60 Hz voltage for a point-to-insulated plane and for a sphere-to-insulated plane at different pressures.

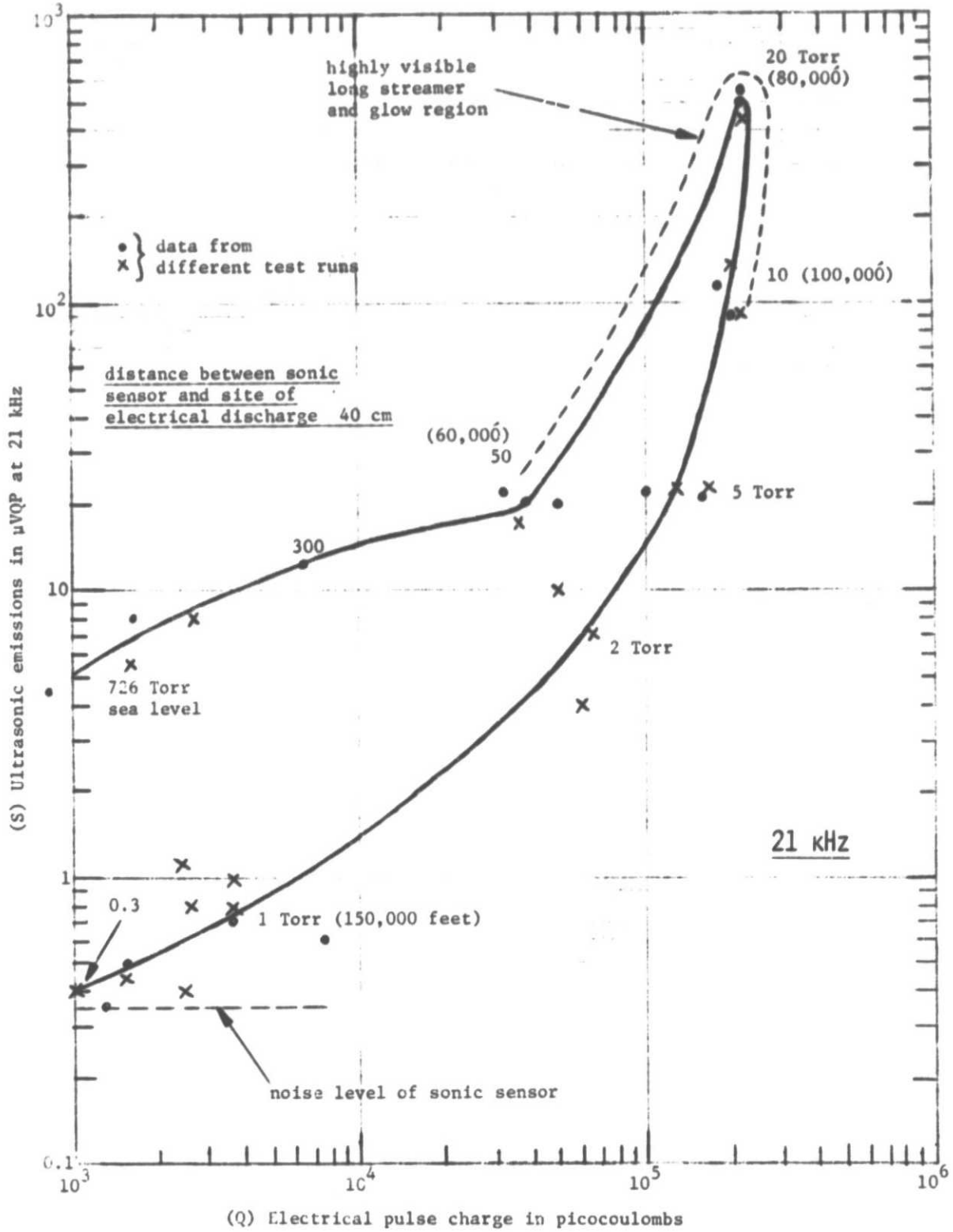

FIG. 3 - Relationship between the ultrasonic (21 kHz) and electrical emissions from a point-to-insulated-plane discharge of 1 mm spacing and stressed at 2.8 KV_{rms} in varying degrees of vacuum

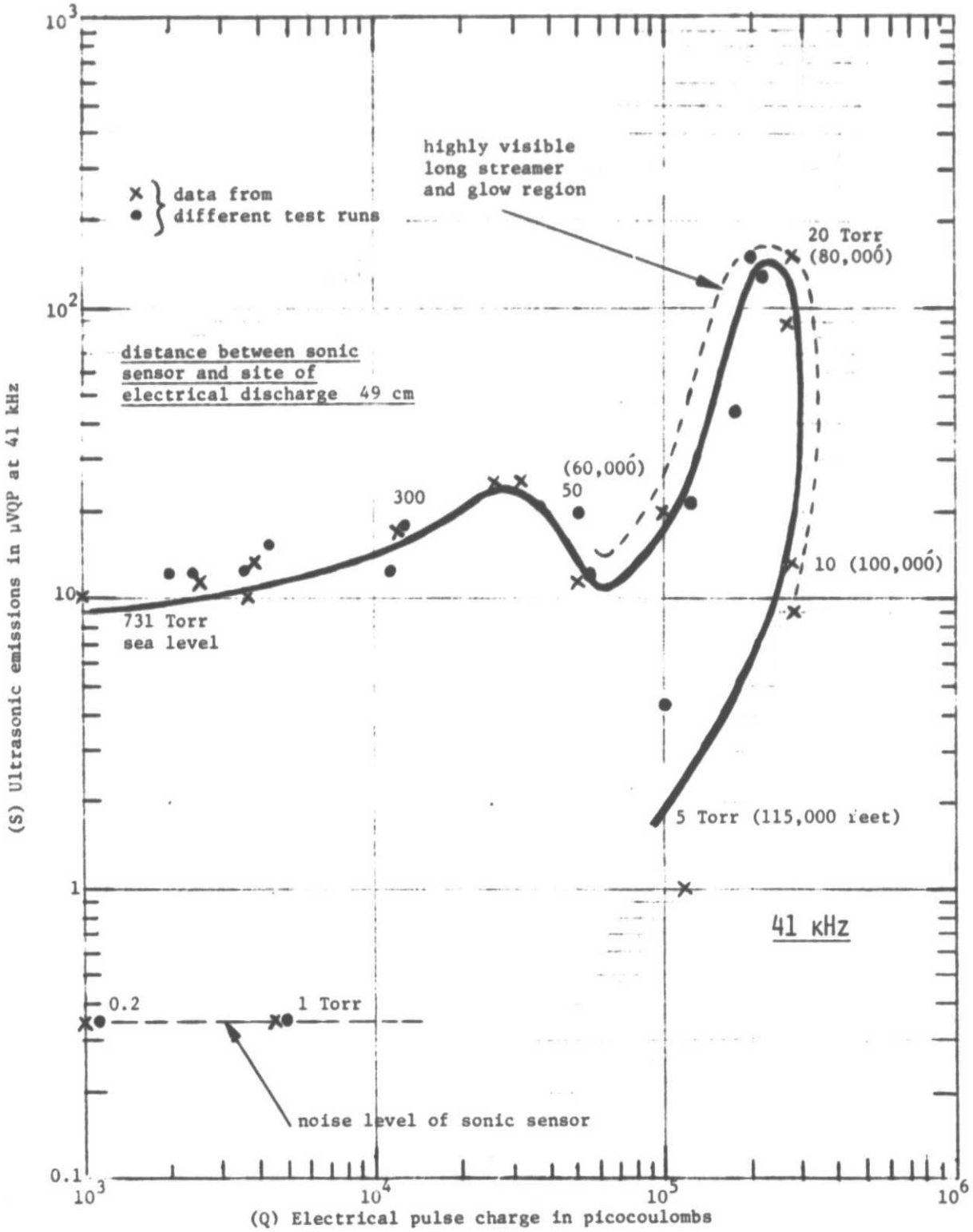

FIG. 4 - Relationship between the ultrasonic (41 kHz) and electrical emissions from a point-to-insulated-plane discharge of 1 mm spacing and stressed at 2.8 KV_{rms} in varying degrees of vacuum

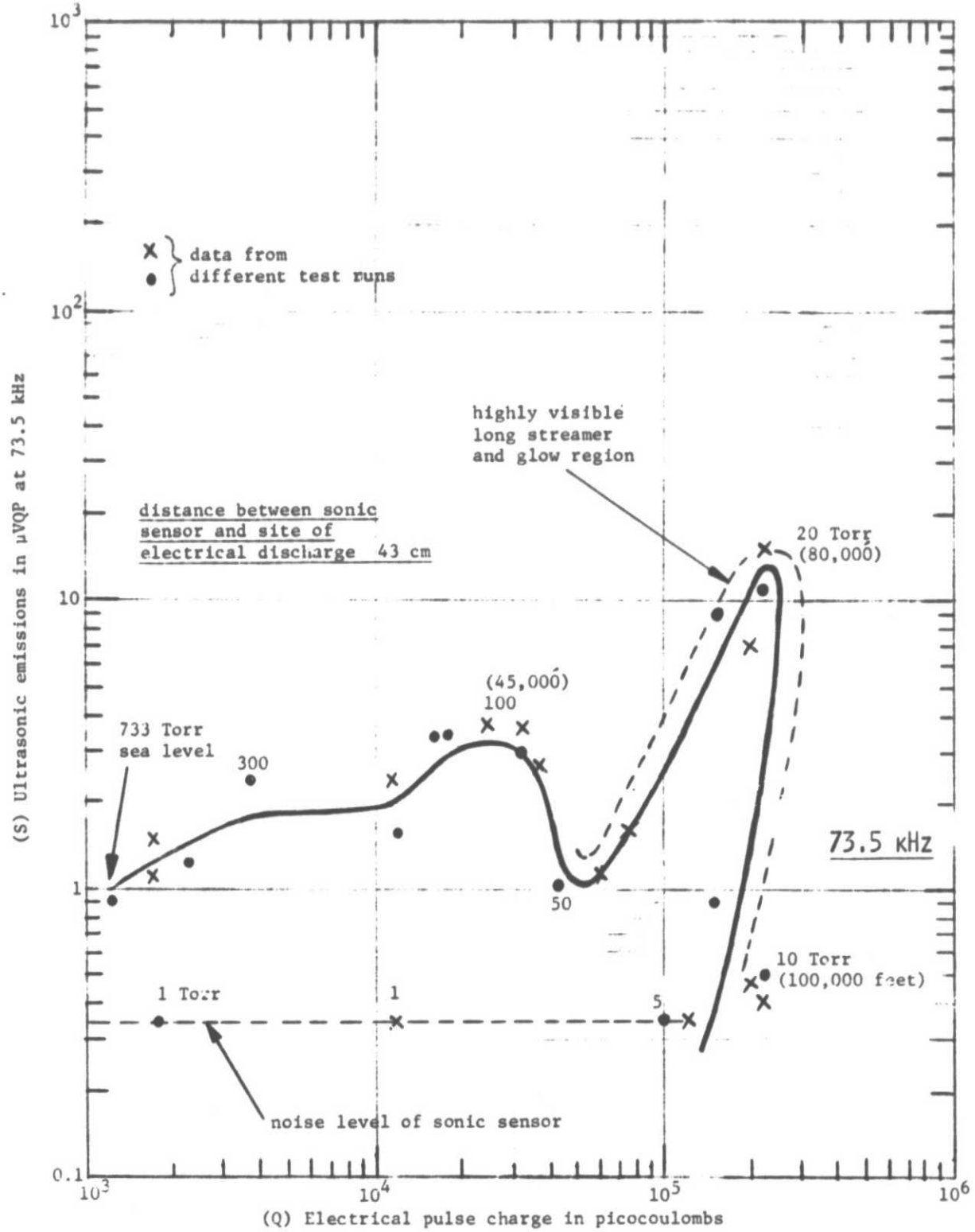

FIG. 5 - Relationship between the ultrasonic (73.5 kHz) and electrical emissions from a point-to-insulated-plane discharge of 1 mm spacing and stressed at 2.8 KV_{rms} in varying degrees of vacuum

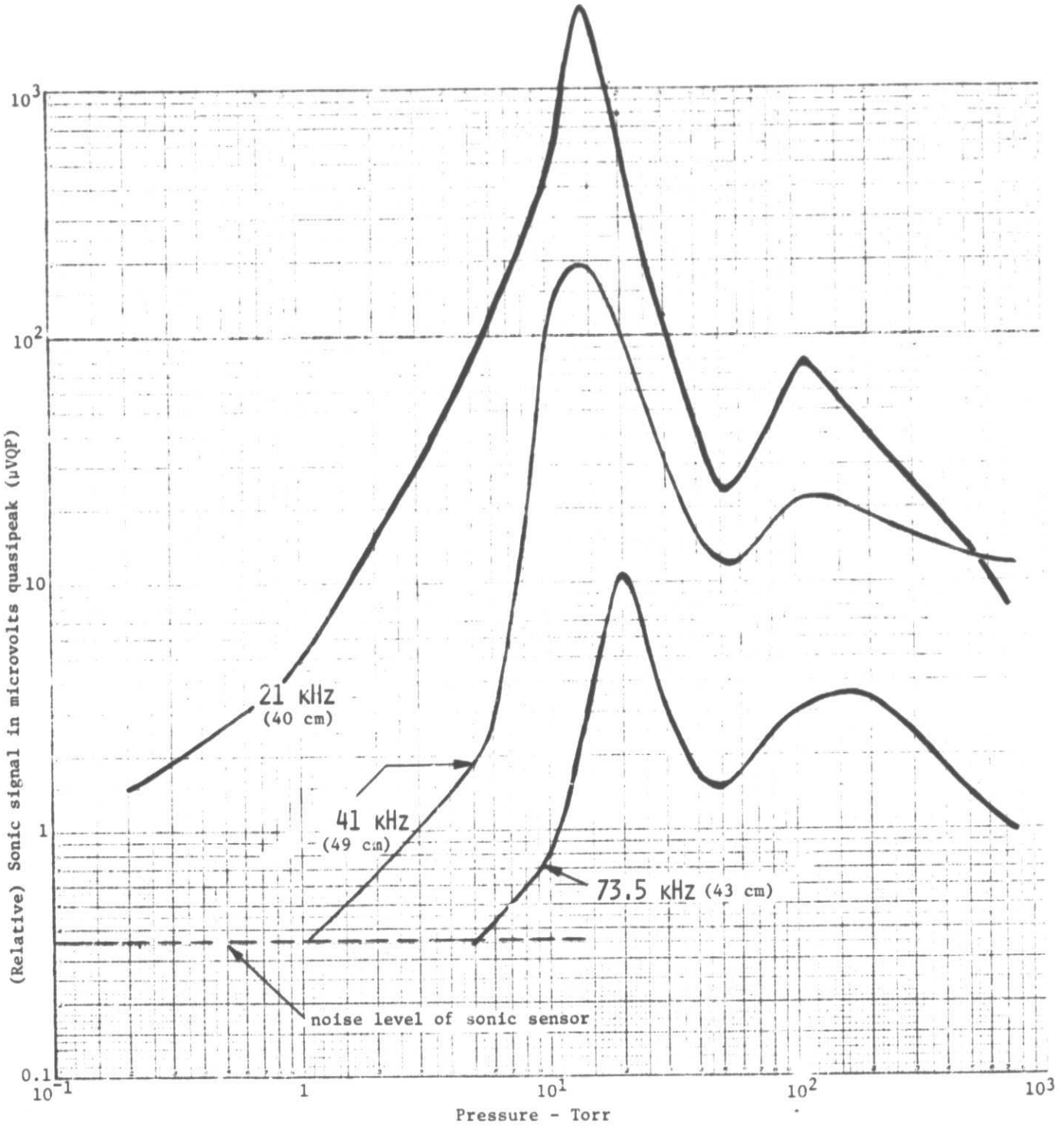

FIG. 6 - Average sonic emissions at 21 kHz, 41 kHz and 73.5 kHz versus pressure for electrical discharges from a point stressed at 2.8 KV_{rms} and spaced 1 mm above an insulated plane

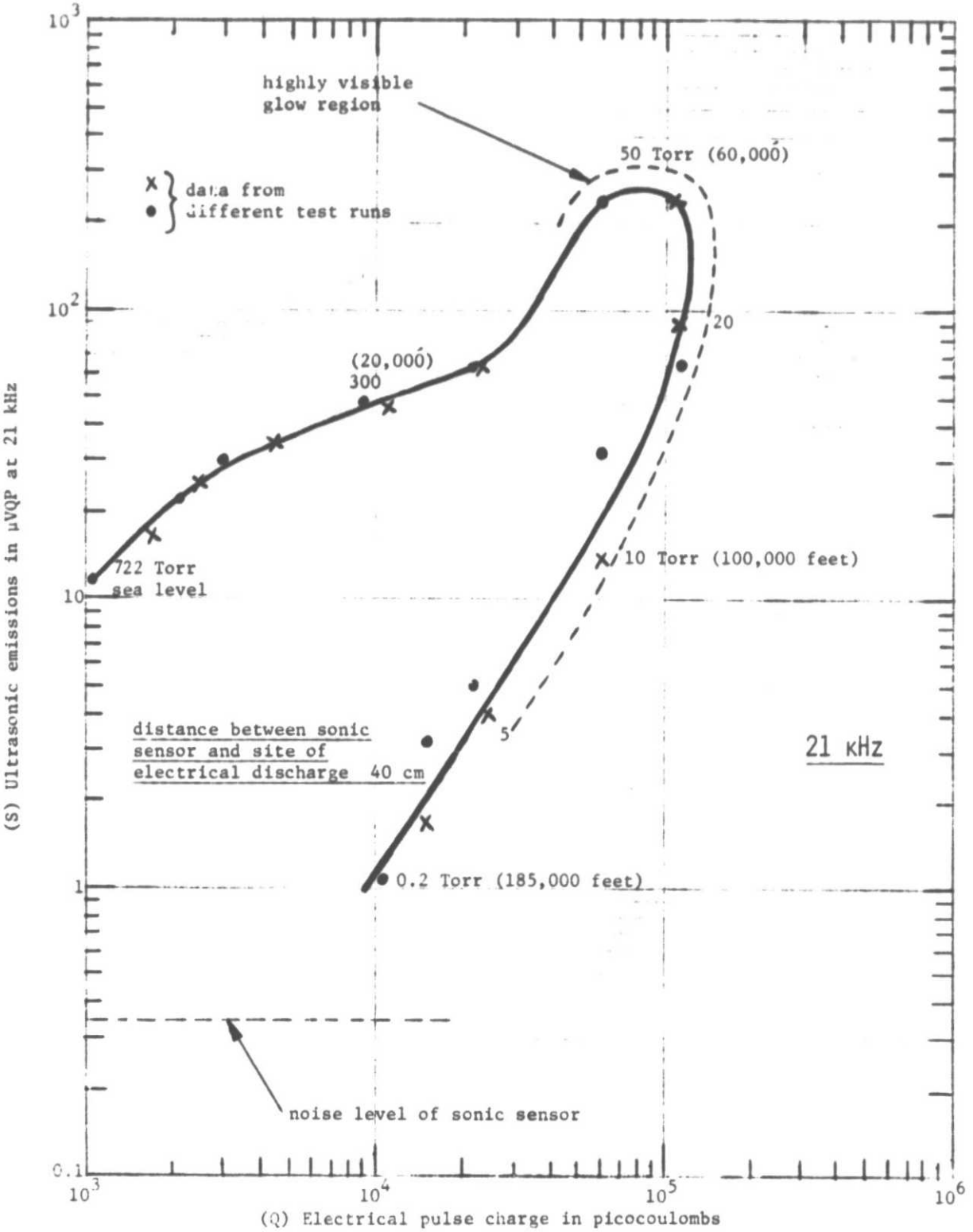

FIG. 7 - Relationship between the ultrasonic (21 kHz) and electrical emissions from a 2.5 cm diameter sphere spaced 0.1 mm from an insulated plane and stressed at 4.2 KV_{rms} in varying degrees of vacuum

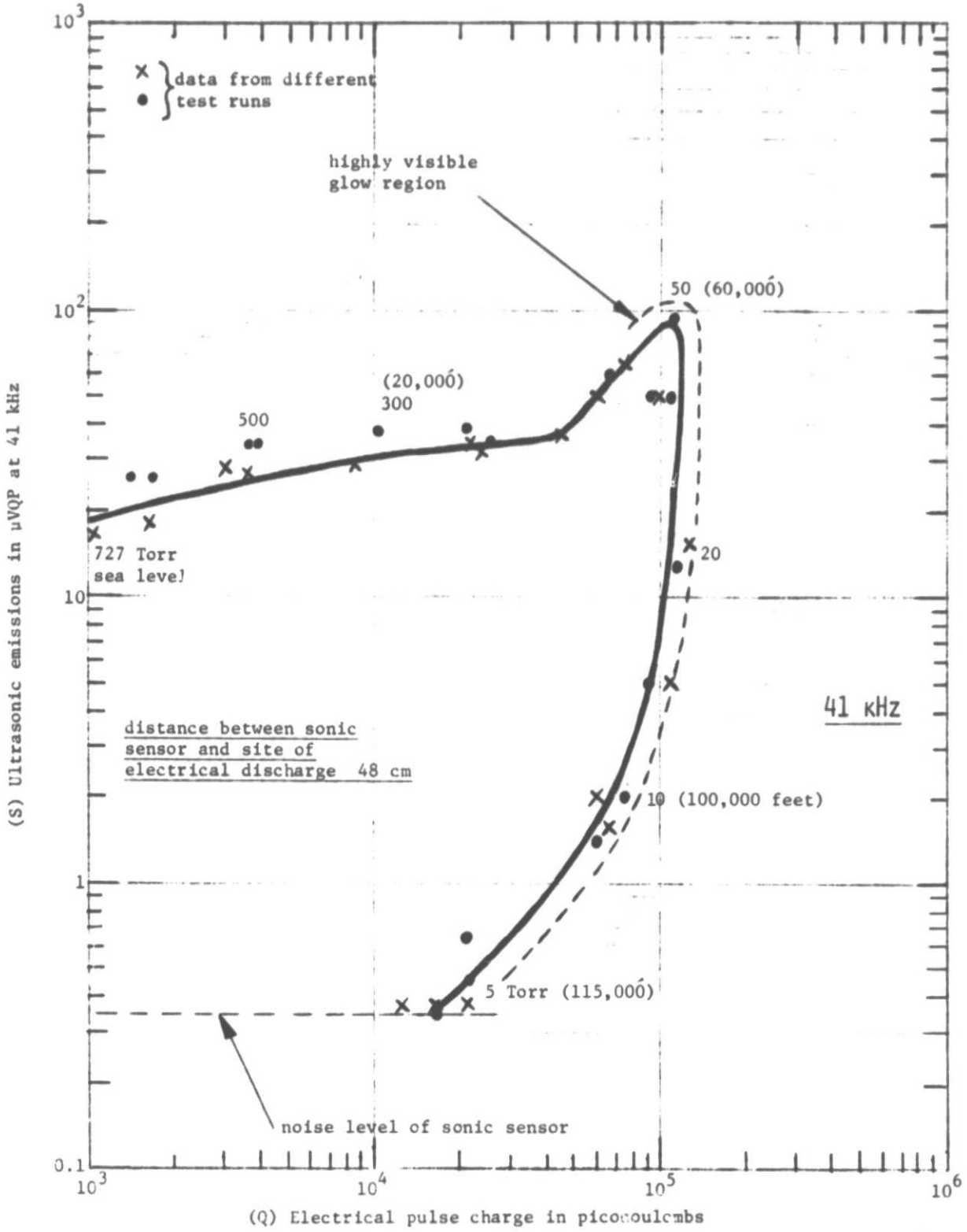

FIG. 8 - Relationship between the ultrasonic (41 kHz) and electrical emissions from a 2.5 cm diameter sphere spaced 0.1 mm from an insulated plane and stressed at 4.2 KV_{rms} in varying degrees of vacuum

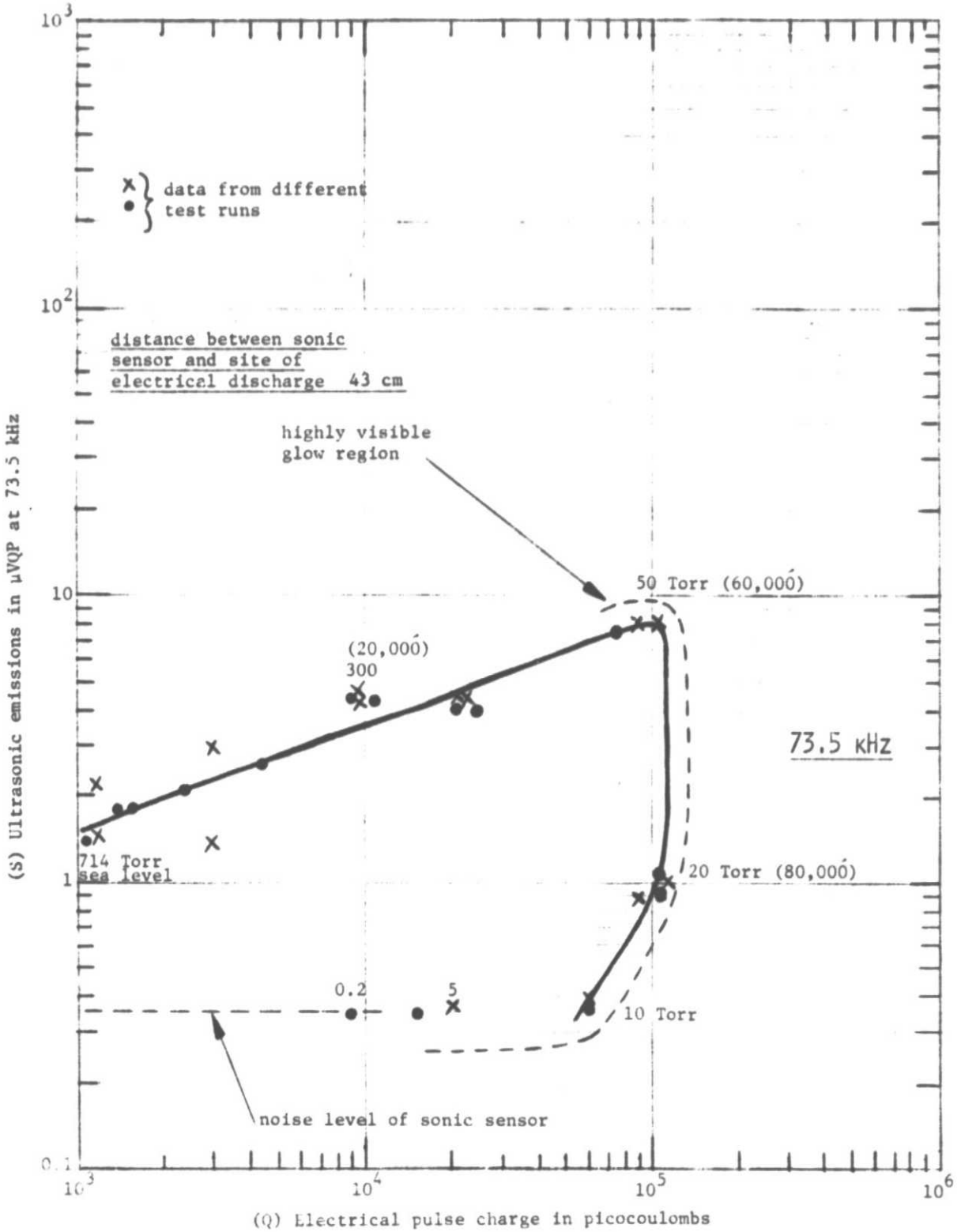

FIG. 9 - Relationship between the ultrasonic (73.5 kHz) and electrical emissions from a 2.5 cm diameter sphere spaced 0.1 mm from an insulated plane and stressed at 4.2 KV_{rms} in varying degrees of vacuum

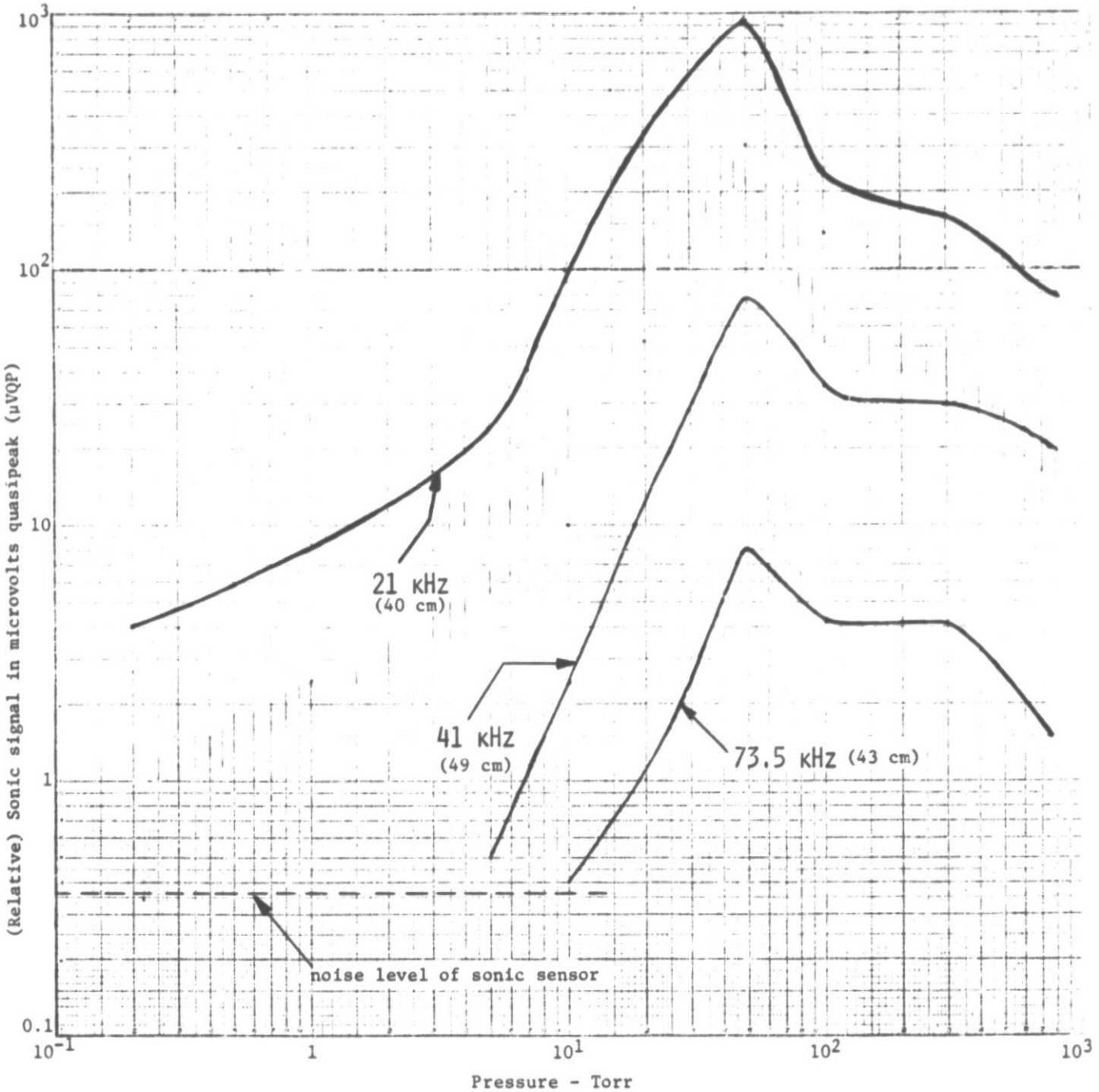

FIG. 10 - Average sonic emissions at 21 kHz, 41 kHz and 73.5 kHz versus pressure for electrical discharges from a 2.5 cm diameter sphere stressed at 4.2 KV_{rms} and spaced C.1 mm above an insulated plane

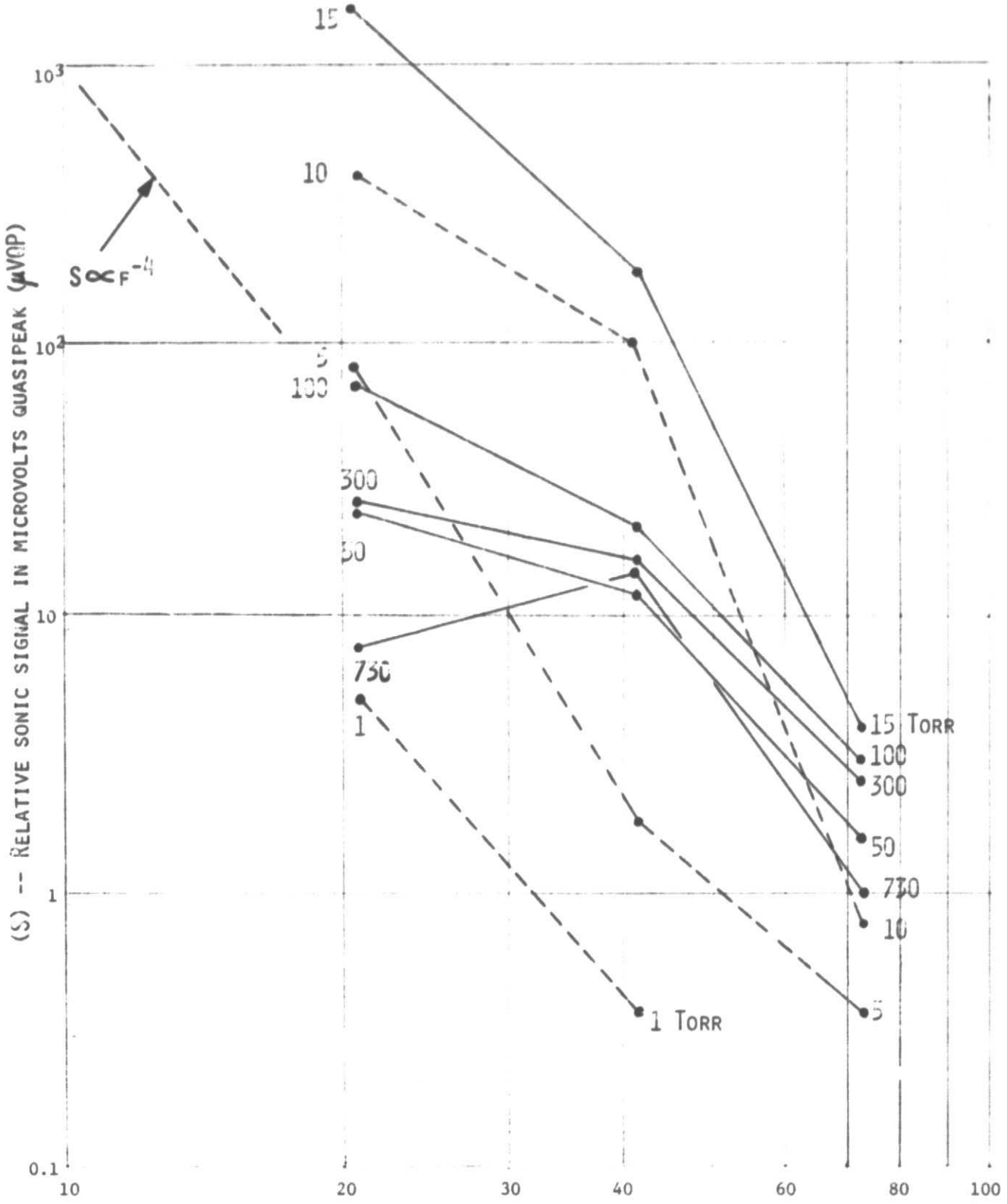

FIGURE 11 -- Frequency spectra of the sonic emissions from discharges from a point stressed at 2.8 kV_{rms} and spaced 1 mm above an insulated plane in varying degrees of vacuum.

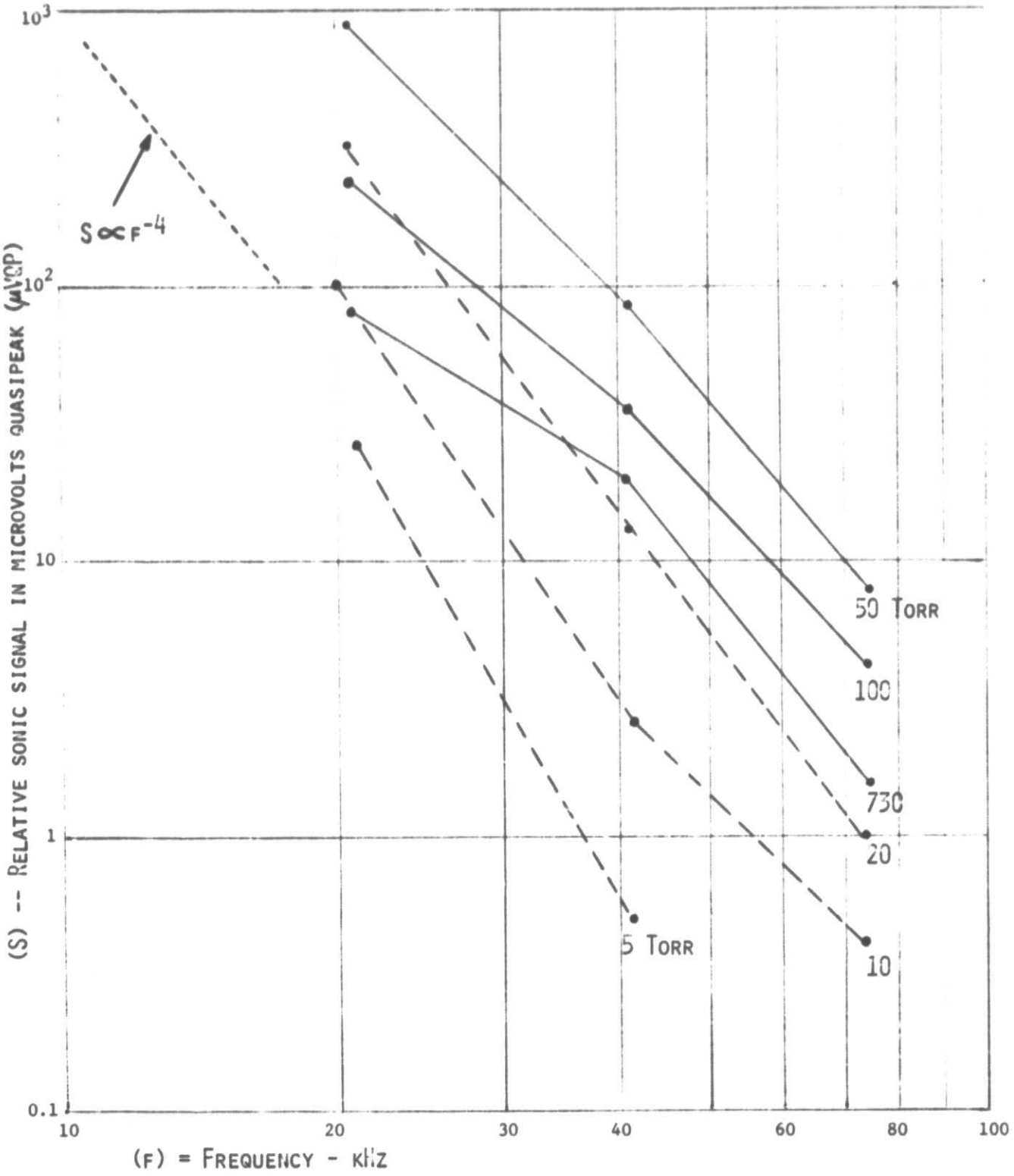

FIGURE 12 -- Frequency spectra of the sonic emissions from discharges from a 2.5 cm diameter sphere stressed at 4.2 kV_{rms} and spaced 0.1 mm above an insulated plane in varying degrees of vacuum

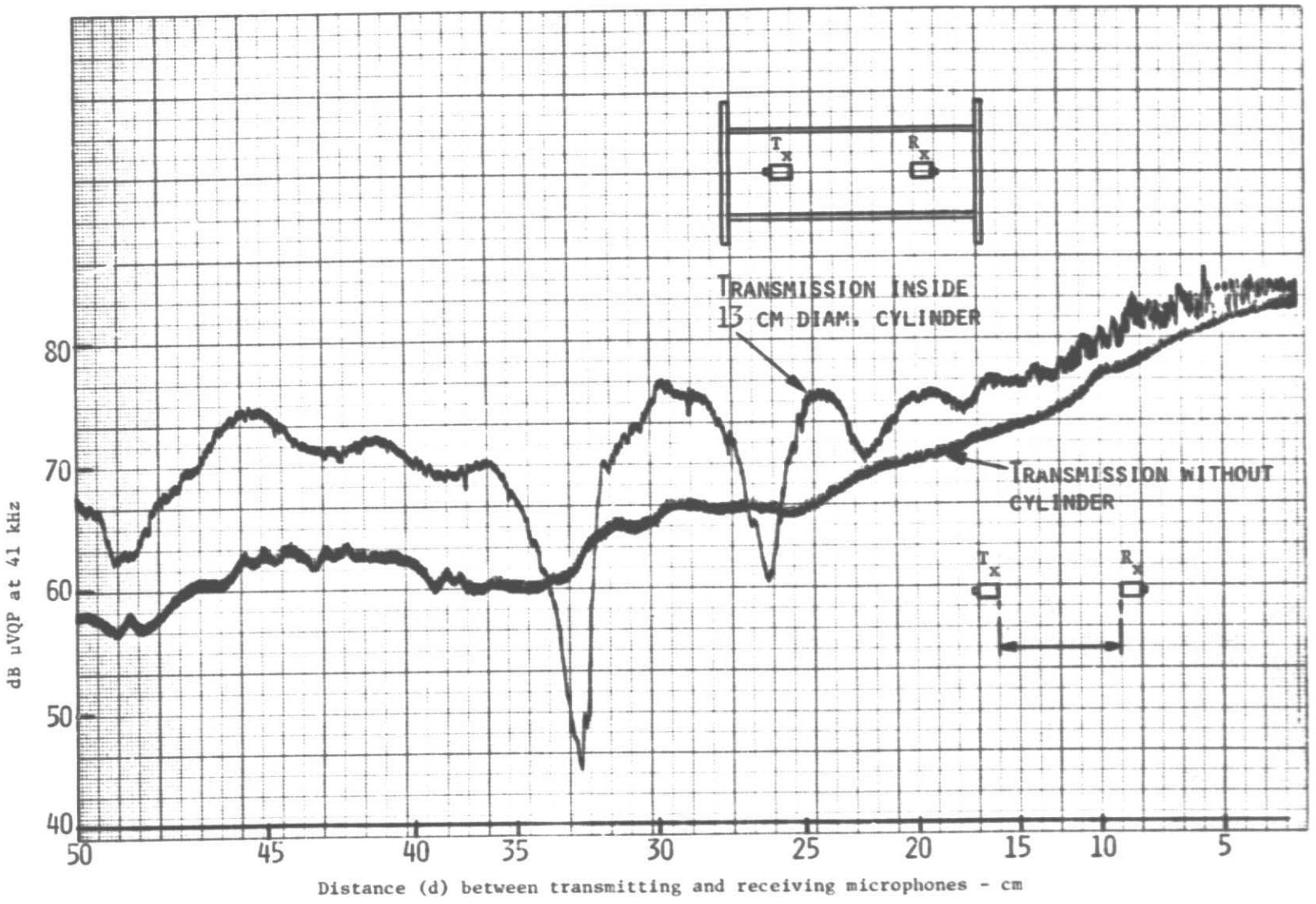

FIG. 13 - ATTENUATION OF 41 KHZ PULSED ULTRASOUND VERSUS DISTANCE IN AIR AT ONE ATMOSPHERE, WITH THE MICROPHONES IN A 13 CM DIAMETER PLEXIGLAS CYLINDER AND WITHOUT A CYLINDER

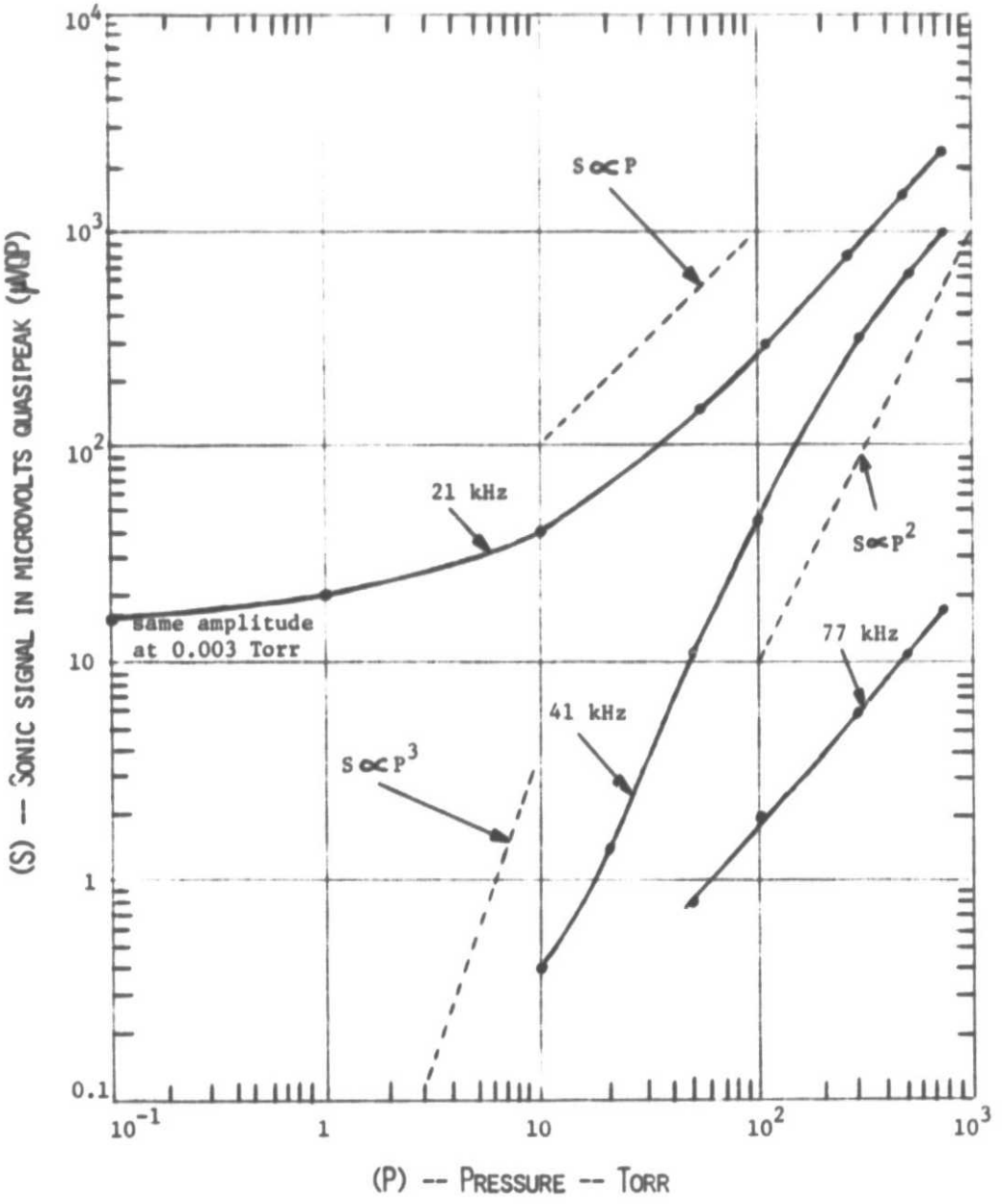

FIGURE 14 -- Response of 21, 41 and 77 kHz sensors versus air pressure when 25 cm from pulsed ultrasound sources of similar microphones activated by 90 volt pulses.

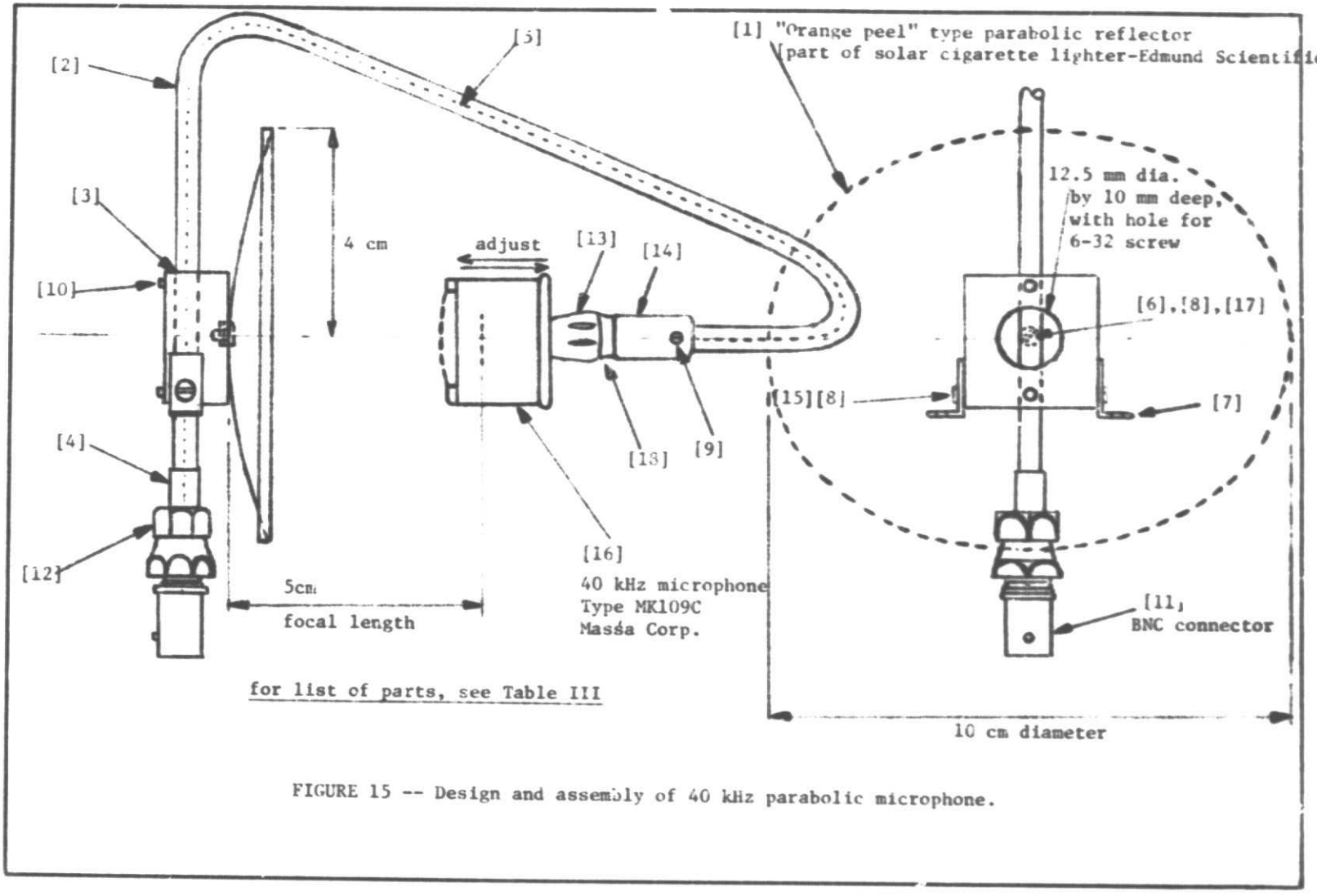

FIGURE 15 -- Design and assembly of 40 kHz parabolic microphone.

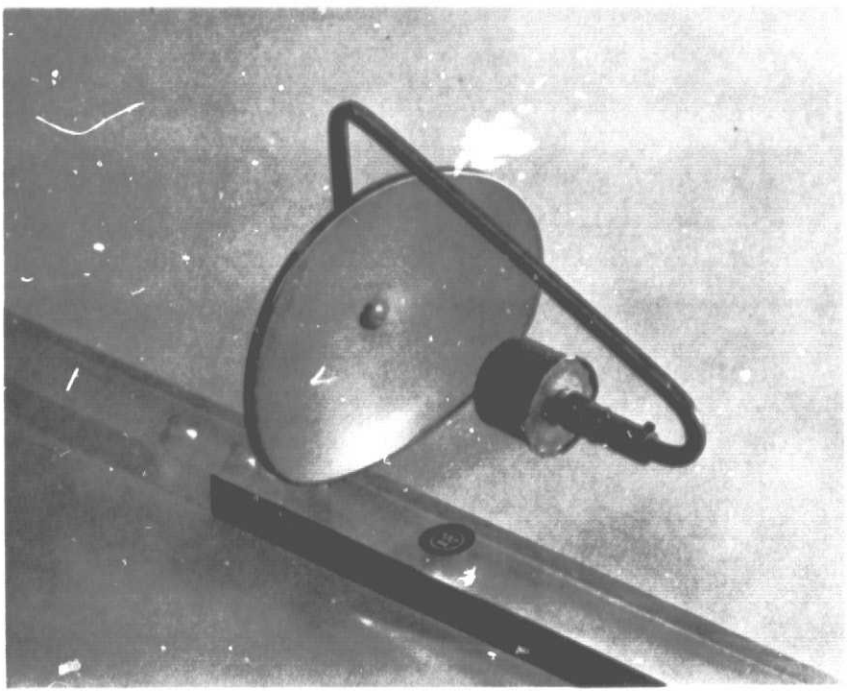

OVERALL VIEW

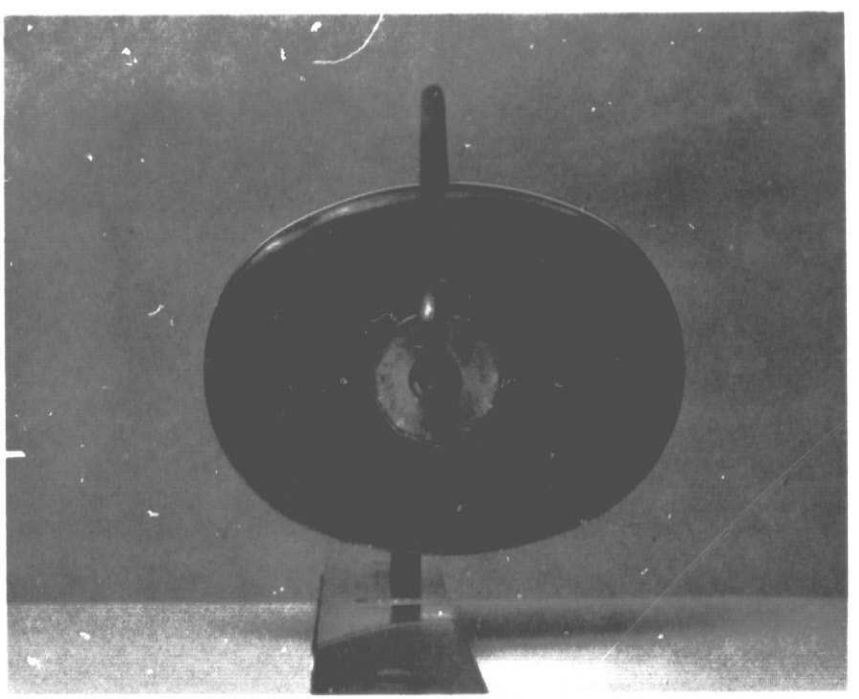

END VIEW

FIGURE 16 -- Views of 41 kHz parabolic microphone.

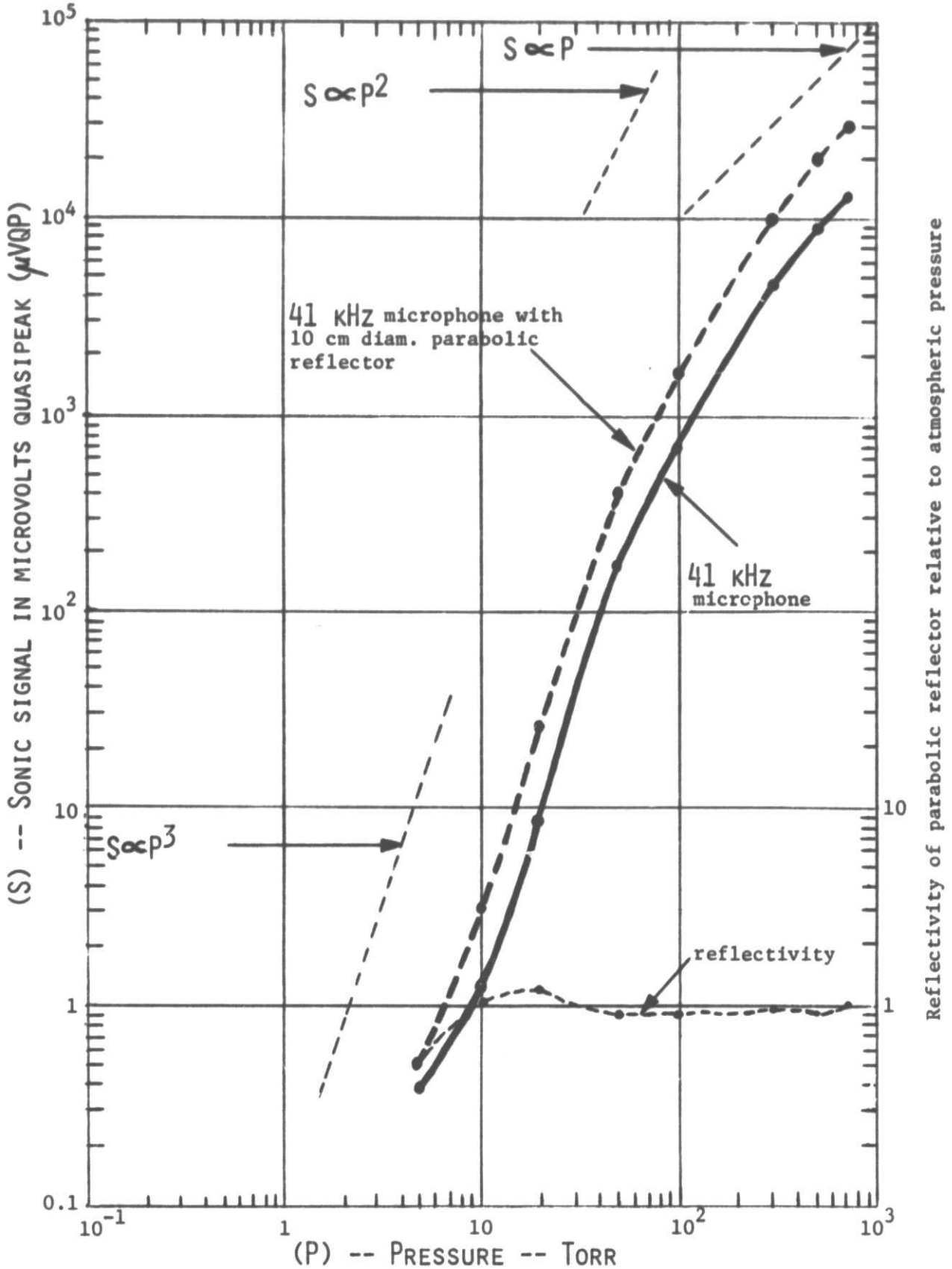

FIGURE 17 -- Response of 41 kHz microphone and 41 kHz microphone with parabolic reflector, versus pressure, when spaced 25 cm (sonic path length) from an 800 volt pulsed 41 kHz narrow beam sonic source.

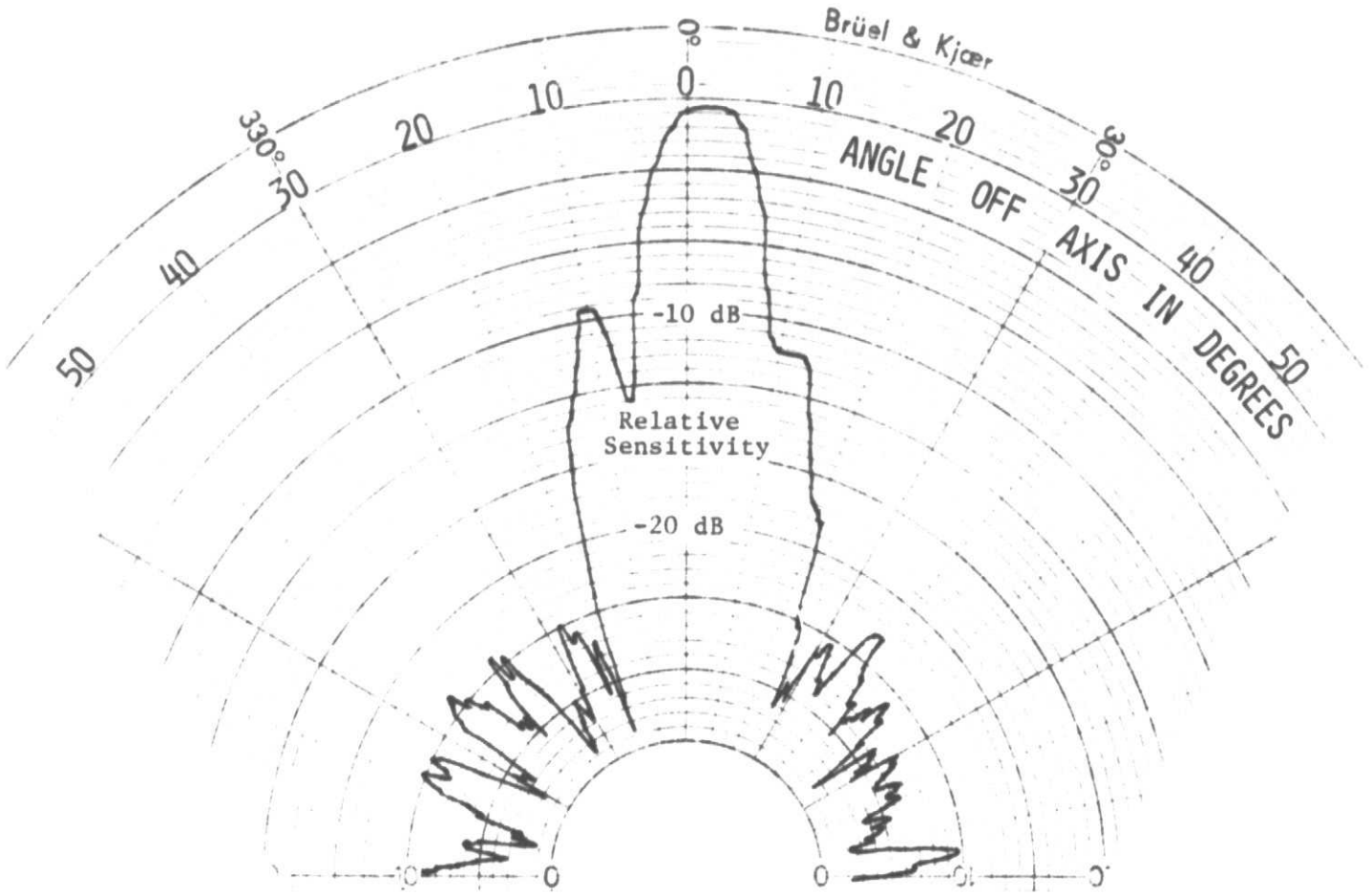

FIG. 18- Directivity of 41 kHz microphone with 10 cm diameter parabolic reflector, measured in air at one atmosphere

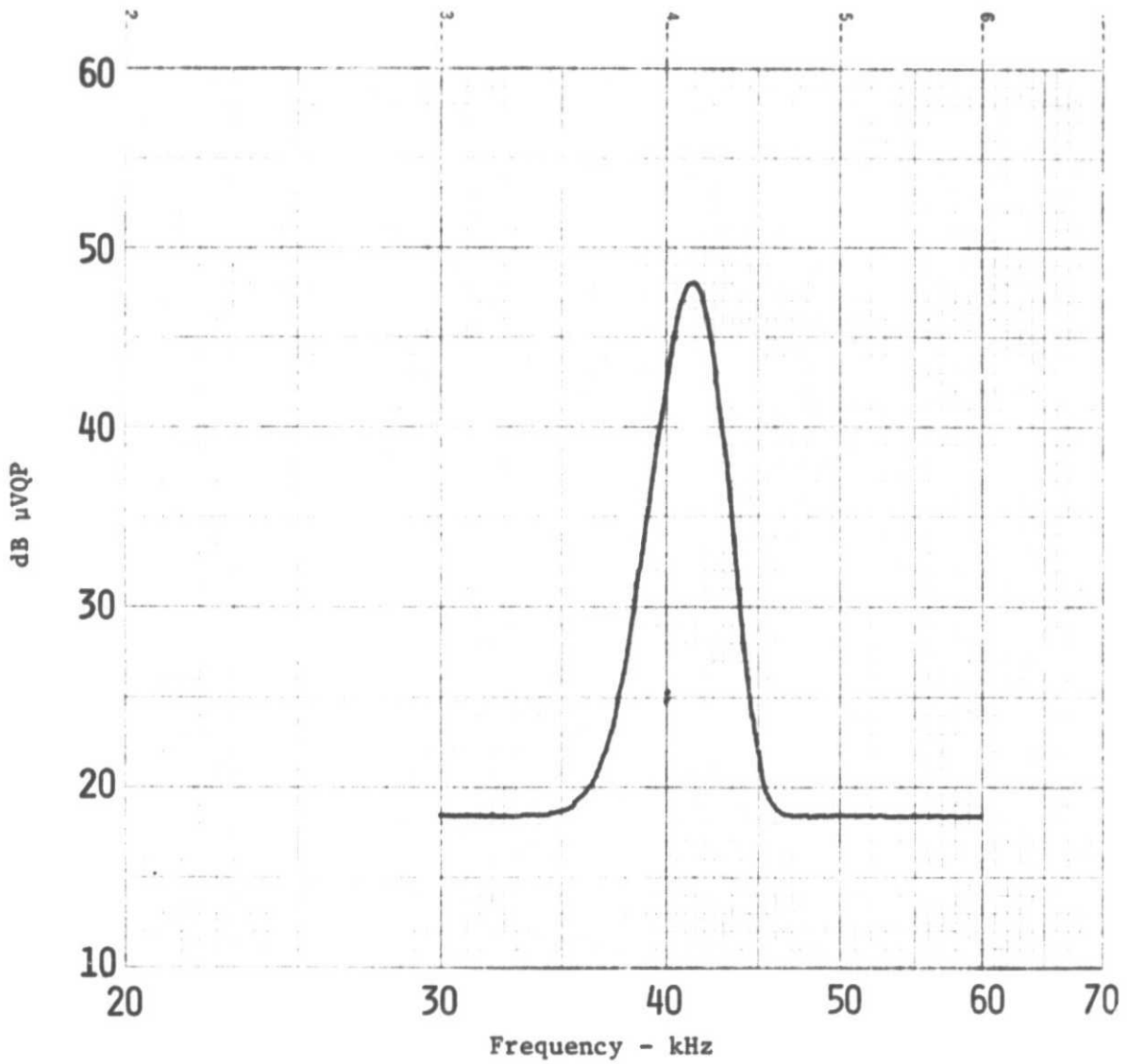

FIG. 19- Frequency response of 41 kHz microphone with 10 cm diameter parabolic reflector

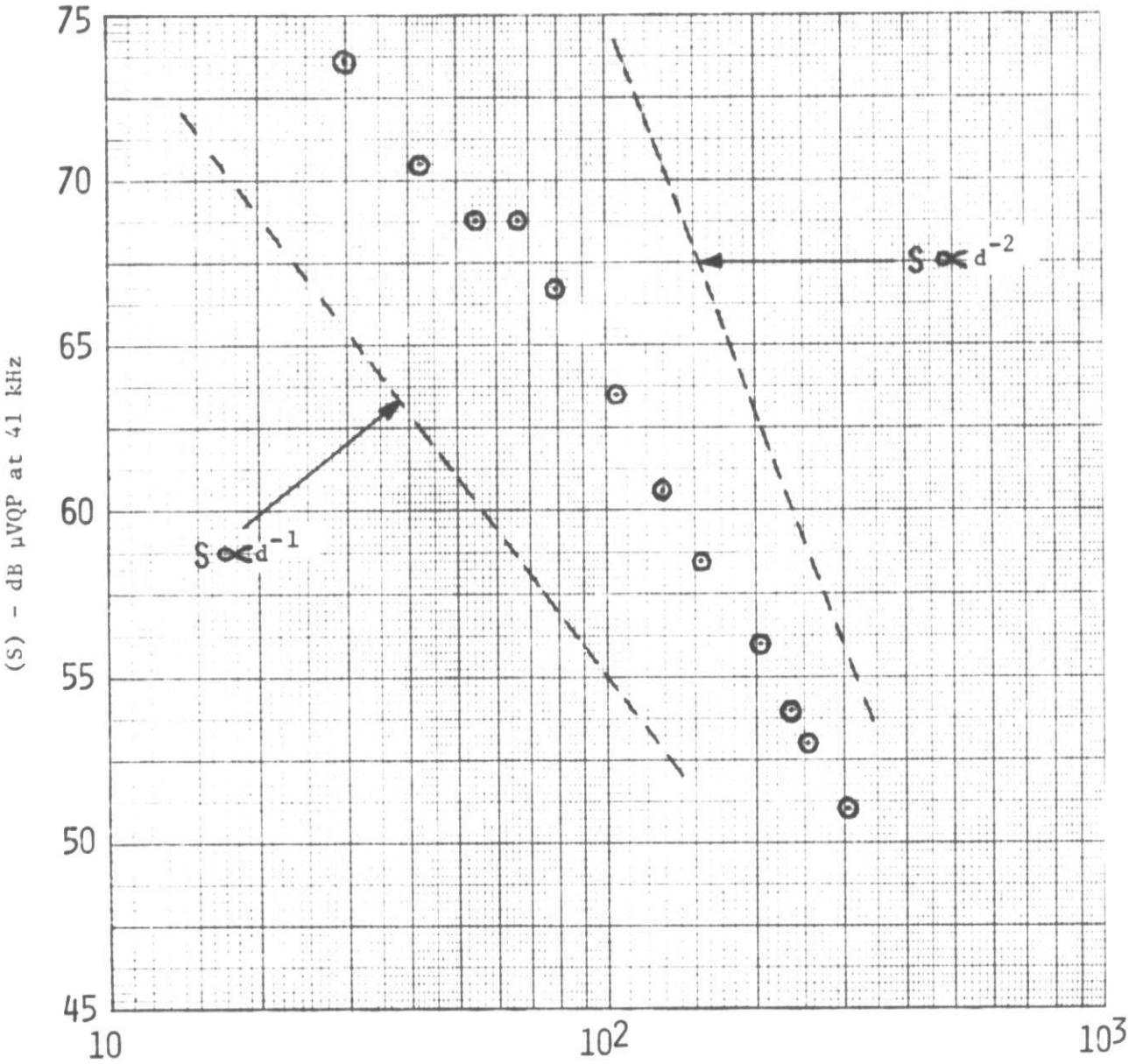

FIG.20 - Attenuation versus distance for 41 kHz sound source measured with 41 kHz microphone and 10 cm diameter parabolic reflector in air at one atmosphere